КИЇВСЬКИЙ
НАЦІОНАЛЬНИЙ УНІВЕРСИТЕТ
ІМЕНІ ТАРАСА ШЕВЧЕНКА

Nicolay Davidenko
Irina Davidenko
Alexander Ishchenko

SPIN-DEPENDENT PROCESSES IN INFORMATION MEDIA BASED ON PHOTOCONDUCTIVE POLYMER COMPOSITES

MINISTRY OF EDUCATION AND SCIENCE OF UKRAINE
TARAS SHEVCHENKO NATIONAL UNIVERSITY OF KYIV

Nicolay Davidenko
Irina Davidenko
Alexander Ishchenko

SPIN-DEPENDENT PROCESSES IN INFORMATION MEDIA BASED ON PHOTOCONDUCTIVE POLYMER COMPOSITES

Monograph

КИЇВСЬКИЙ ВІТЛ УНІВЕРСИТЕТ 2020

161. N. A. Davidenko, I. I. Davidenko, I. A. Savchenko, et al. J. Appl. Phys. 103 (2008) 094223.

162. T. Yoshimura Thin-Film Organic Photonics: Molecular Layer Deposition and Applications. Boca Raton – London – New York: CRC Press, 2011.

163. I. Naydenova (Ed.). Holograms – Recording materials and applications. Intech: Rijeka, Croatia, 2011.

164. A. Priimagi, A. Shevchenko. J. Polymer Science. Part B: Polymer Physics. 52 (2014) 163.

165. X. Wang. Azo Polymers. Synthesis, Functions and Applications. Berlin Heidelberg: Springer-Verlag, 2017.

166. I. I. Davidenko. App. Opt. 12 (2016) B133.

167. A. N. Simonov, D. V. Uraev, S. G. Kostromin, et al. Laser Physics. 16 (2002) 1294.

168. C. Cojocariu, P. Rochon. Macromolecules. 38 (2005) 9526.

169. N. A. Davidenko, I. I. Davidenko, V. A. Pavlov, et al. Theor. Exp. Chem. 52 (2016) P.298.

170. N. A. Davidenko, I. I. Davidenko, E. V. Mokrinskaya, et al. Theor. Exp. Chem. 53 (2017) 100.

171. https://www.youtube.com/watch?v=ZTi_S0-aTQ8.

CONTENTS

Навчальне видання

ДАВИДЕНКО Ірина Іванівна
ДАВИДЕНКО Микола Олександрович
ІЩЕНКО Олександр Олександрович

СПІН-ЗАЛЕЖНІ ЕФЕКТИ У ФОТОАКТИВНИХ ПОЛІМЕРНИХ КОМПОЗИТАХ

Монографія

(Англійською мовою)

Оригінал-макет виготовлено ВПЦ "Київський університет"

Формат 60x84$^{1/16}$. Ум. друк. арк. 10,64. Наклад 100. Зам. № 220-9882.
Гарнітура Times New Roman. Папір офсетний. Друк офсетний. Вид. № Х5.
Підписано до друку 07.12.2020

Видавець і виготовлювач
ВПЦ "Київський університет"
Б-р Тараса Шевченка, 14, м. Київ, 01601, Україна
☎ (38044) 239 32 22; (38044) 239 31 72; тел./факс (38044) 239 31 28
e-mail: vpc_div.chief@univ.net.ua; redaktor@univ.net.ua
http: vpc.univ.kiev.ua
Свідоцтво суб'єкта видавничої справи ДК № 1103 від 31.10.02

UDC 544.52:66.095.26
D26

Reviewers:
Prof. V. A. Skryshevsky
(*Institute of High Technologies of Kyiv Taras Shevchenko National University, Kyiv*)
Corresponding Member of the NAS of Ukraine, Prof. V. M. Ogenko
(*V.I. Vernadsky Institute of General and Inorganic Chemistry of the NAS of Ukraine*)

Recommended to print
by the Academic Council of the Chemical Department
(protocol № 2 from 23 October 2019)

Approved
by the Academic Council of Kyiv Taras Shevchenko National University
(protocol № 3-19/20 from 26 December 2019

Davidenko N.
D26 Spin-dependent processes in information media based on photoconductive polymer composites : Monograph. / N. A. Davidenko, I. I. Davidenko, A. A. Ishchenko. – K. : Publishing and Polygraphic Center "Kyiv University", 2020. – 182 p.

ISBN 978-966-933-116-8

The results of the investigation of spin-dependent processes in photoconductive polymer film composites with various sensitizers used in information technology for recording, storing, and processing optical information are summarized. Special examples of the manifestation of such processes and their relationship with the molecular structure of the components of composites are discussed. It is emphasized that photogeneration, recombination, and transport of non-equilibrium charge carriers are spin-dependent in photoconductive polymer composites.

UDC 544.52:66.095.26

ISBN ISBN 978-966-933-116-8

INTRODUCTION

This book mainly uses the results of experiments that have been carried out by the authors and collaborators for many years. The book is aimed at drawing the attention on the importance of choice of components of photoactive composites from polymers and dopants, for example, organic dyes, for their use in information technologies (molecular electronics, spintronics, holography) and in solar energetic. The book consists of 2 sections.

The first section shows the effect of the structure of the components of the composites on the internal photoeffect. The main attention is paid to the spin-dependent interaction between the components of the composites in the internal photoeffect. Various compositions of dopants of composites are considered.

The second section discusses the practical applications of photoactive polymer composites. The possibilities of using photoactive polymer composites in holographic interferometry are demonstrated.

The book is recommended for use in educational institutions that have courses in chemical physics, physical chemistry, optics, physics of semiconductors and dielectrics.

CHAPTER ONE
Spin-dependent processes in information media based on photoconductive polymer composites

In modern information technologies, organic photoactive materials including nanocomposite materials [1–21] are widely used. Among them, a large class of media based on thin photoconductive film polymer composites (FPC) occupies a worthy place, the properties and applications of them are described in numerous reviews [22–39]. The key moment in the photoconductivity is the effect of photogeneration, i.e. the formation under the light influence of free, moving in an external electric field, and not interacting with each other in the volume of the FPC carriers of electric charge. In most cases, the FPC consists of a polymer binder and dopants such as organic dyes or related compounds. With all the variety of known and newly synthesized organic compounds, some of which can form thin films and others absorbing the light, the choice of compounds to produce photoconductive FPCs is a separate scientific task, because not always intense light absorption is accompanied by effective photogeneration. This is caused by the probability of electronic transitions between excited photogeneration centers and molecules along which transport of nonequilibrium carriers occurs. Similar to crystalline and amorphous semiconductors [40], non-equilibrium charge carriers (electrons and holes) move in the space between degenerate energy states, but at the same time in disordered FPCs such states are localized on individual molecules or their fragments. Therefore, radical-ions correspond to non-equilibrium charge carriers. At small distances between localized states at which

unpaired electrons are present, it becomes necessary to consider the various possibilities of interaction of such unpaired electrons both with similar electrons and with the electron-nuclear system of the localized states. Thus, the photogeneration, recombination, and transport of non-equilibrium charge carriers in FPC in the general case are spin-dependent. At present, a large number of experimental results have been accumulated, and adequate model concepts on spin-dependent photophysical processes in organic materials have been proposed, in particular, in FPC for information media [41–50]. One of the prospects for the application of such materials is the rapidly developing spintronics [51–61]. However, review papers devoted to spin-dependent processes in organic materials are not available at present. This review is focused on these issues. It analyzes and summarizes the regularities of photogeneration and transport of charge carriers in FPC, which were not previously formulated in a key reflecting the FPC feature in the state of aggregation and in the form of a true solid solution of molecules.

1.1. Model of photoconductive polymer composite

Practically used FPCs are characterized by the absence of translational symmetry in the distribution of molecules. From the point of view of the disorder model, their structure corresponds to the solid solution [62–65]. In general, this is a true solution of the three types of compounds in a neutral film-forming binder. The molecules of the two compounds in the solid solution form zones of electron and/or hole transport, and the molecules of the third compound are centers of photogeneration and/or recombination of charge carriers. Fig. 1.1 shows schematically a diagram of the zones of electron and hole transport, as well as the electronic levels of photogeneration centers [64] in samples of practically used FPC. In Fig. 1.1, 1 – is the electron transport zone, formed by LUMO molecules with acceptor properties that are at a distance of $R_n = N_a^{-1/3}$ from each other (N_a is the concentration of these molecules in FPC), 2 – is the zone of hole

transport, formed by HOMO of molecules with donor properties at a distance of $R_p = N_d^{-1/3}$ from each other (N_d is the concentration of these molecules in FPC), 3 – is the photogeneration and recombination centers, which are represented by two molecules. As a rule, structures for FPCs investigations and their application contain a solid substrate of dielectric material with successively deposited layers of electrically conductive contact 1 with electron work function E_{F1}, FPC with thickness L, and electrically conductive contact 2 with work function E_{F2}. Sometimes (for example, in electrography and holography [63]), contact 2 is absent and its role for creating an external electric field in an FPC plays an electric charge of ions deposited on the FPC surface using a corona gas discharge.

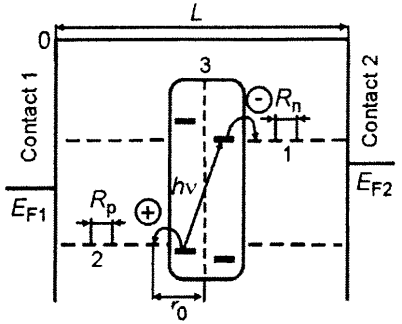

Fig. 1.1. Diagram of energy levels in the sample with FPC and electrical contacts

The electron levels of the molecules forming the transport zone are not split and remain local, but the wave functions of the molecules and their ions partially overlap. The localization radii of the wave functions of [66–68] electrons (α_n) on acceptor molecules and holes (α_p) on donor molecules may differ. The transfer of charge carriers in the transport zone occurs as a result of tunnel transitions between local levels of molecules. For most practical FPCs, an empirically established [69–74] dependency of mobility (velocity in an electric unit field) of electrons (μ_n) and holes (μ_p) in the corresponding transport zones on the external electric field strength (E) and temperature (T) is typical:

$$\mu_n \sim R_n^2 \exp(-2R_n/\alpha_n) \exp(-(W_{0n} - \beta E^{1/2})(T^{-1} - T^{-1}_0)/k_B), \quad (1.1)$$

$$\mu_p \sim R_p^2 \exp(-2R_p/\alpha_p) \exp(-(W_{0p} - \beta E^{1/2})(T^{-1} - T^{-1}_0)/k_B), \quad (1.2)$$

where W_{0n} and W_{0p} are the activation energies of the electron and hole mobility at E = 0, β is the coefficient numerically coinciding with the Poole-Frenkel constant [74], k_B is the Boltzmann constant, T_0 is the temperature at which the experimental graphs of $\lg(\mu_n)$ and $\lg(\mu_p)$ on T^{-1}, extrapolated to high temperatures T, measured for different values of field strength E, intersect.

In Fig. 1.1, photogeneration centers for generality are presented consisting of two parts, to emphasize that during photogeneration excitation, when a quantum hν absorbs a photogeneration center, either the complete transfer of an electron between molecules or the electron density redistribution and its concentration in one of the parts of the excited dye molecule occurs [75, 76]. The first case takes place in intermolecular complexes with charge transfer (CCT) [77], or between donor and acceptor parts of molecules, for example, in compounds with intramolecular charge transfer (CICT) [78, 79]. When a light quantum is absorbed by the photogeneration center, the electron and the hole are separated and can leave the photogeneration center, passe into the corresponding transport zone, forme a Coulomb-bounded (geminal) electron-hole pair (EHP) with an initial distance r_0 between the charges (Fig. 1.1). The quantum yield (η_0) of the formation of EHP is determined by the intramolecular conversion and interconversion of the photogeneration center molecule, as well as by the ratio of the energies of the HOMO and LUMO of this center with the energies of the corresponding molecular orbitals of the molecules forming the electron and hole transport zones. The charge carriers in the EHP can then either disperse over long distances, thereby creating free non-equilibrium photoconductivity carriers, or recombine at the center of photogeneration. For the practically used FPCs, the quantum yield (η) of photogeneration of free charge carriers can be represented by the empirical dependency [64]:

$$\eta \sim \eta_0 R_n R_p \exp(-R_n/\alpha_n - R_p/\alpha_p) \exp(-(W_{0ph} - \beta E^{1/2})(T^{-1} - T^{-1}_0)/k_B), \quad (1.3)$$

where $W_{0ph} = e^2/\varepsilon r_0$ is the activation energy of the photogeneration of free charge carriers at E = 0 (e is the electron charge, ε is the dielectric constant, r_0 is the initial distance between the charges in the EHP), T_0 is the temperature at which experimental graphs of $\lg(\eta)$ versus T^{-1} for different E, extrapolated to large T, intersect. It should be noted that within the framework of the two-stage process of photogeneration of

carriers through the formation of an EHP and its dissociation, the value of W_{OPH} can be associated with the energy of the Coulomb interaction between an electron and a hole in an EHP. Non-equilibrium charge carriers moving in the direction of the collecting contacts can be captured into local energy states (traps). Traps are formed as follows: for holes – by molecules with an ionization potential lower than the ionization potential of molecules from the hole transport zone, for electrons – by molecules with an electron affinity energy greater electron affinity energy for molecules from the electron transport zone, and molecules with a large dipole moment or localized electrical charge. Besides, non-equilibrium charge carriers photogenerated at different photogeneration centers or injected from electrical contacts can converge near the photogeneration/recombination center, thereby forming a contact charge pair, and recombine with each other at this center. The presented scheme of photogeneration, transport, and recombination of charge carriers in FPCs very closely reflects the real situation, but it is sufficient to reveal significant differences from crystalline and amorphous glassy semiconductors.

In this review, much attention is paid to the FPCs with a hole-type conductivity, since it is for them experience is accumulated in using as information media, in particular, as electrographic and holographic media [80–85]. These FPCs were tested in holographic recording media (GRM) for the photothermoplastic (FTP) method for recording optical information. For these applications, GRM must be selective to a specific spectral composition, given by the working wavelength of the used laser radiation. The advantage of selective HRM is that during the registration of holograms it is more protected from external illumination, and therefore can be used in conditions without special protection of the optical scheme from solar and another lighting. HRM for PTP method of holograms recording should have the necessary rheological properties, high electrical resistance in the dark, and great photoconductivity. So far, oligomers or cooligomers with hole conductivity [80–85] have been used in such HRMs. To create photosensitive information media, hetero-chain electron-donor oligomers were synthesized and used. This made it possible to create photothermoplastic recording media with optimal rheological properties. The absence of a highly elastic state in oligomers makes it possible almost instantaneously to transfer the film from a solid

glassy state to a liquid state with low viscosity and vice versa. This makes it possible to reduce the development time to microseconds and work almost in real time. In this case, the film must have sufficient elasticity for use on a flexible substrate. Such forced elasticity below the glass transition temperature can be achieved only due to the conformational transitions of individual oligomer units containing, as a rule, donor multi-core conjugate substituents. The most known among them is the tri-nuclear 9-carbazolyl.

The principle of holographic recording using the FTP method [80] is shown in Fig. 1.2.

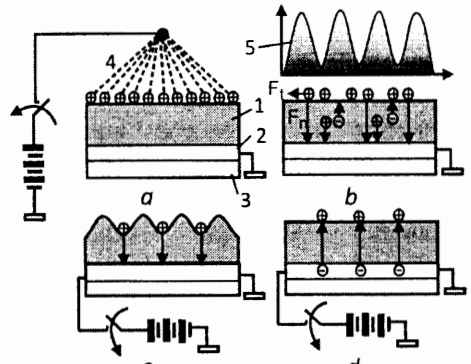

Fig. 1.2. Scheme of the PTP method of holographic recording:
a – charging the FPC surface in the corona discharge; *b* – irradiation of the FPC surface with spatially modulated light; *c* – development of the hologram; *d* – erasing the hologram. 1 – is the transparent solid substrate; 2 – is the transparent electrically conductive layer; 3 – is the FPC; 4 – is the corona electrode; 5 – is the light intensity I, modulated through the X coordinate

For the application of the PTP recording method use HRM based on photoconductive FPC and electronic devices controlling its operation [80–85]. The HRM consists of three layers (Fig. 1.2): the bottom layer 1 is a glass or lavsan substrate, the middle layer 2 is a transparent electrically conductive film (usually SnO_2: In_2O_3 films are used – ITO), the top layer 3 is FPC. The functioning of the HRM at the holographic registration consists of three stages. Before holographic recording, the surface of the FPC is charged in a corona discharge (Fig. 1.2*a*), for example, with positive ions. During the hologram registration

(Fig. 1.2, *b*), the electrons reaching the surface of the charged film neutralize the positive ions on the surface, and the spatial distribution of the light intensity is converted to the spatial distribution of the density of the surface electric charge. This results in the spatial distribution of normal (F_n) and tangential (F_t) electrostatic forces. For the development of a latent electrostatic image of a hologram (Fig. 1.2, *c*) an impulse of electric current is passed through a transparent electrically conductive ITO film. As a result, it heats up and heats FPC to softening temperature. In real devices, the heating velocity reaches 10^6 °C/s. In this case, the electrostatic forces F_n and F_t deform the free surface of the FPC and the latent electrostatic image is transformed into a geometric relief of the film surface (Fig. 1.2, c). After cooling the film, the geometric relief is conserved for a long time. In a real HRM, a recorded hologram can conserve for decades at temperatures not exceeding the softening temperature of the FPC and not lower than the temperature of mechanical destruction (cracking). To erase the hologram, it is enough to pass a current pulse with a duration longer than the duration of the hologram development current pulse through the ITO film (Fig. 1.2, *d*). In this case, the FPC is heated to temperatures above the softening temperature, and the geometric relief disappears. After cooling the FPC to room temperature, it can be used to re-record the hologram. The number of cycles of recording-erasing holograms can be several hundred or even thousands.

Optimal functioning conditions for FPC [80] in preparation for registration, during registration, during the development and erasure of holograms provides an electronic device for recording holograms. This is reached as follows.

1. In the corona discharge, the surface of the FPC is charged at the optimum value of the charging current to the maximum possible value of the charging potential. In this case, there should be no destruction of the FPC surface and no local breakdowns.

2. Registration of a hologram and the formation of a latent electrostatic image of a hologram occurs over time, which is determined by the holographic sensitivity of the HRM and the intensity of the reference beam.

3. The development of a latent electrostatic image is carried out at the optimum temperature rise velocity for which chaotic "frost" deformations which are the main source of noise in a holographic image do not have time to develop. The maximum possible spatial frequency band of the transfer characteristic is achieved. The optimum velocity of temperature rise is realized because pulsed heating of the FPC with a speed > 10^5 °C/s occurs from the optimum constant value of the initial temperature to the pre-set value of the diffraction efficiency measured in the first diffraction order. This is determined by the universality of the holographic recording system which does not depend on the optical scheme for the formation of holograms. Such a process can be realized with the help of an electrical circuit for setting up an optimal initial temperature of the HRM, an electrical circuit for development of a latent electrostatic image, an optoelectric circuit for limiting the development process upon reaching a given diffraction efficiency value.

4. The erasing of the developed image of the hologram is carried out to reuse the HRM. At the stage of erasing the hologram, the duration of the current pulse is longer than the duration of the hologram development pulse ensures the heating of the FPC to a higher temperature, and leads to the alignment of the FPC surface. Thus, the HRM and the electronic control unit are a single system each element of which operates taking into account the characteristics of the other.

As a result of the studies of electric and photophysical processes in the FPC, effective HRM for the PTP method of information recording [80–88] have now been created and are being practically applied. The low information noise of the reconstructed images of holograms (Fig. 1.3, Fig. 1.4) allowed them to be used not only in artistic holography (Fig. 1.4, Fig. 1.5) but also in the methods of holographic interferometry, may indicate the high information properties of the HRM.

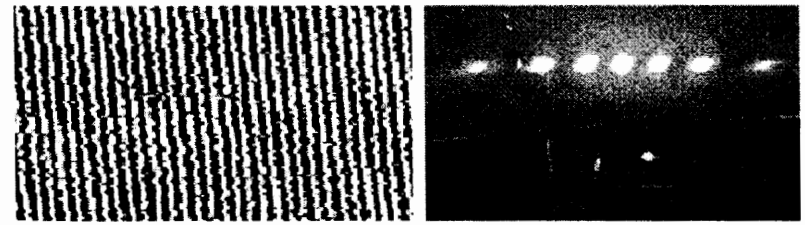

(*a*) (*b*)

Fig. 1.3. Photograph of the section of the FPC surface after recording a hologram of a plane wavefront in the HRM (*a*) and a photo of the screen on which the holographic image of the plane wavefront (*b*) is projected

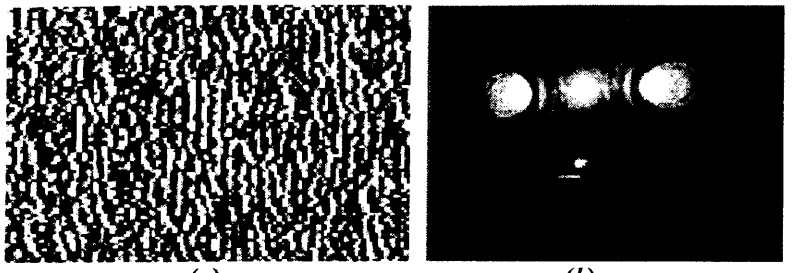

(*a*) (*b*)

Fig. 1.4. Photograph of the section of the FPC surface after recording a hologram of the coin in the HRM (*a*) and a photograph of the screen on which the holographic image of the coin (*b*) is projected

Fig. 1.5. Photograph of the screen on which the holographic image of the car layout is projected

HRMs have a wide range of practical applications, in particular, in holographic interferometry to determine the refractive index and/or its changes under the influence of various factors [80–88]. Since it is very difficult to determine small changes in the refractive index by usual optical methods, in these cases holographic interferometry methods are most effective. This has a promising application in the investigations of the kinetics of photochemical reactions in biology and medicine [89, 90]. In these applications, it is often important not only to accurately measure changes in the refractive index (**n**) but especially to use very carefully probing light sources with intense radiation. Therefore, one of the important requirements for HRM is high photosensitivity at the wavelength of the used laser. This task is partially resolved using the FPC for the PTP method of holograms recording. For example, in [86–88] it is shown that another promising direction in the use of holographic interferometry methods is the

study of photochemical reactions. An example of using this method is described in [86, 87]. Images of interference patterns for the experiment with the Methylene Blue dye solution are shown in Fig. 1.6. It can be clearly seen that with an increase in the time of exposure of laser radiation (Fig. 1.6, *a*–*e*), the number of interference fringes increases meaning a change in the refractive index (Δn) of the dye solution in the region of this effect. After turning off the laser, the refractive index is restored (Fig. 1.6, *e*–*k*). In [86, 87] from the analysis of a series of such experiments, conclusions were made about the occurrence of photochemical reactions in the investigated objects.

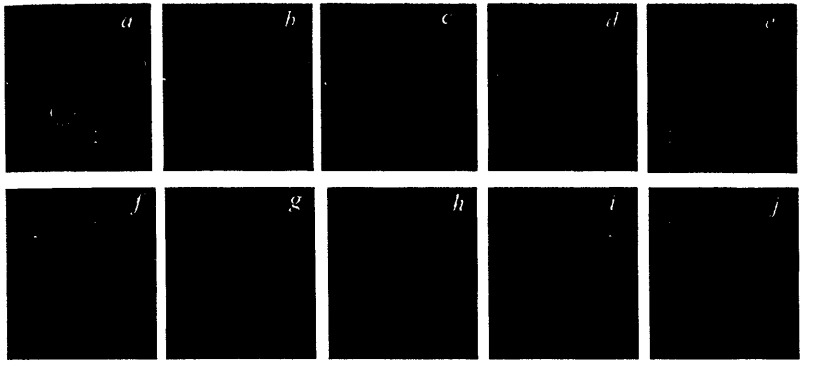

Fig. 1.6. Images of interference patterns for the experiment with the Methylene Blue dye solution under laser irradiation with λ_{irr} = 667.5 nm for 2 s (*a*) 10 s (*b*), 30 s (*c*), 50 s (*d*) and 65 s (*e*) and after it is turned off after 5 s (*f*), 10 s (*g*), 20 s (*h*) 30 s (*i*) 60 s (*j*)

This method of studying the kinetics of photothermal and photochemical reactions is very informative and illustrative. Fig. 1.7 shows the plot Δn(t) which was obtained [86] using the interferogram image processing technique (Fig. 1.6). The measurement results have enough high accuracy (~10^5) which is very satisfactory for practical use.

Thus, numerous examples of practical applications of FPC in holographic interferometry (as one of the applications) (Fig. 1.7) show the importance of further research and the development of fundamental knowledge about the basic processes in them. Some results will be discussed in the following sections of this paper.

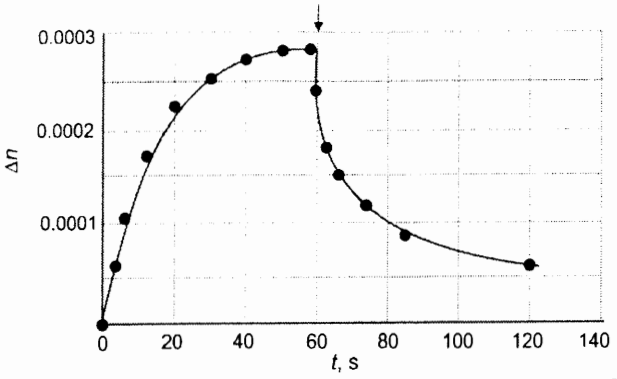

Fig. 1.7. Dependency Δn(t) of the cuvette with an aqueous solution of the dye after turning on the laser with λ_{irr} = 667.5 nm at time t = 0 and after turning off the laser at time t = 60 s (time off light is indicated by the vertical arrow)

1.2. Electronic transport

Let us briefly consider the main electronic processes determining the photoelectric properties of the FPC which are necessary for their practical application in information media: photogeneration, recombination, transport, and charge carrier capture. The regularities of transport of charge carriers in FPC differ significantly from those in ordered organic solids and in glassy inorganic materials. The mobility of electrons and holes for the majority of FPCs does not exceed 10^{-4} $m^2/(V \cdot s)$ [69–74, 91–93] imposing a restriction on the choice of experimental methods for studying electron transport. In studies, the focus is on the dependencies of μ_n and μ_p on E, T, L, N_a, N_d. Numerous investigations have established that the experimental dependences of electron transport for the majority of FPCs are satisfactorily described by dependencies (1) and (2). However, a common point of view to explain these dependencies has not yet been developed.

This is connected with various model considerations explaining the experimentally observed dependencies (1.1) and (1.2). There are common and alternative factors and examples. For example, in explaining the dependency of the electron mobility on the field

strength E and temperature T, one can use the Onsager model [94, 95] the analytical representation of which at a high external electric field strength corresponds to the Poole-Frenkel [96] model since in real FPC impurity centers cannot be excluded. They already have an electric charge or it appears as a result of their thermofield ionization since due to an external electric field in the process of experiments [71]. Besides, the effect on the movement of free charge carriers of the dipole moments of molecules [96, 97] being the part of the FPC should be taken into account.

Within the framework of such representations, the parameter T_0 in (1.1) and (1.2) is associated with features of the Coulomb centers (for example, with their temperature of destruction) controlling the transport of non-equilibrium carriers, or with features of diffusion and tunneling carrier transport in strong electric fields near the Coulomb centers. However, to explain the dependencies (1.1) and (1.2), only the idea of the amorphous FPC state is sufficient, i.e. the idea of the energy and spatial disordering of local centers from the corresponding charge carrier transport zones. Since the transport of charge carriers between individual molecules or fragments of the polymer chain being the part of the FPC occurs as a result of tunnel junctions, it is impossible not to take into account that the probability of a separate charge carrier jump significantly depends on the distance between molecules, steric factors, molecular vibrations, and the difference between energies of LUMO (for electrons) and HOMO (for holes) of these molecules [98–102]. Therefore, the effect of field strength E and temperature T is reduced to the facilitation of intermolecular electronic transitions. Due to the dispersion of distances and the energies of the molecules, the integral mobility of the charge carrier packet corresponds to dependencies (1.1) and (1.2).

In polymer matrices, the use of long-range order representations is generally not entirely correct, but from the standpoint of the cluster model, one can assume the existence of a correlation in the spatial and energy distribution of molecules along which transport occurs. Then, we can talk about the legality of the existence of the discussed model representations. Besides, partial anisotropy in the distribution of the energy states of molecules in the direction of movement of non-equilibrium charge carriers in the FPC can occur when an external

electric field is applied due to the polarization of the electron shells of these molecules. This is confirmed, in particular, by the influence of an external electric field on the distribution of the electron density of the HOMO of organic dyes as can be seen from the changes in their optical absorption spectra [79, 103–108]. Thus, in electronic transport, even through non-polar molecules, the external electric field "brings about order" in the distribution and makes this transport quasi-one-dimensional which reveals itself in dependencies (1.1) and (1.2).

We also note here that taking into account changes in the electron density distribution under the influence of an external electric field can be useful in further improving the theoretical model concepts of electronic transport. The unidirectional shift of the electron density in a real organic molecule should be accompanied by an increase of the influence of positively charged atomic nuclei from which the outflow of electron density occurs. Such field-induced positive and negative charges can interact with non-equilibrium carriers and by the nature of their effect on transport are similar to Coulomb centers. Thus, for a significant increase in the speed of movement of non-equilibrium charge carriers in the FPC, the transport zones should contain molecules (or fragments of the polymer chain) with a minimum and preferably regular distance from each other, without additional links increasing steric difficulties during π-electron transitions.

Besides, these molecules or fragments of the polymer chain should have as many delocalized boundary molecular orbitals as possible, but with a small dipole moment. The condition for minimizing the dipole moment of molecules, as well as the absence of electric charges of molecular fragments or ions, is determined by the need to level the influence of the Coulomb centers on the transport. Fulfillment of the specified conditions when selecting components of the FPC while achieving sufficient chemical purity and structural homogeneity is an important factor in creating transport and photogeneration FPC. It should be noted that FPC samples with high features of electron transport may not necessarily have photoconductive properties. Therefore, we now dwell in greater detail on the features of photogeneration of charge carriers.

1.3. Photogeneration of charge carriers

Molecular media (both organic crystals and polymer films with low molecular weight additives) are solid-state systems that are formed due to intermolecular interaction. The intramolecular structure of covalently bounded atoms in a molecule and in a crystal, or the structure of a complex with charge transfer (CCT), formed due to donor-acceptor (D-A) interaction, practically does not change when a solid is formed. Depending on the electronic structure of the molecule, the energy of intermolecular interaction can vary widely from 10^{-3} eV (for Van der Waals interaction) to units of eV (in the case of D-A bond).

The formation of a CCT or polymer doping with other sensitizers, for example, with dyes is determined by intermolecular interaction forces: Van der Waals, Coulomb, dipole-dipole, polarization, induction, and others. A complex with charge transfer can be formed at small distances between donor and acceptor molecules (~ 0.35 nm [75,109]) and their orientation providing the most efficient overlap of their orbitals leading to the formation of a D-A complex or a CCT. Such formation is connected with the redistribution of electron density due to electron transfer from the donor's HUMO to the acceptor's LUMO [75]. Depending on whether a partial or full charge transfer occurs in the ground or in the excited state of the complex, the complexes are divided into strong (ion-radical salts), weak and so-called contact ones.

According to the quantum chemical theory [110–112], the intermolecular D-A interaction occurs due to the quantum-mechanical mixing of two states: non-polar (DA) when only the Van der Waals interaction takes place between the donor and acceptor molecules, and the polar D^+A^- when the electron is transferred from the donor to the acceptor. The average D-A energy W_{DA} of the interaction is determined by the integral of the resonance of the polar and non-polar components, and the mixed state actually described by the dipole $D^{\delta+}A^{\delta-}$ where $0 \le \delta \le 1$ is the degree of charge transfer. According to the value of the energy within the range 0.05–1.0 eV, the intermolecular D-A interaction (inside the complex) lies between the covalent bond (units of eV) and the hydrogen bond

(0.05–0.5 eV) and the Van der Waals bond (10^{-4}–10^{-1} eV) connections. A generalized energy diagram of D-A systems of various types is shown in Fig. 1.8, where RIS are the radical ion salts, CCT are the charge transfer complexes, CC are the contact complexes; E_0 is the main level, $E_S^{(i)}$ is the singlet excited state, $E_T^{(i)}$ is the triplet level, W_0 is the state of the nonpolar CCT component, W_1 is the state of the CCT polar component (D^+A^-), I_d is the ionization potential of the donor molecule, A_a is the electron affinity of the acceptor molecule. On its base, on the difference in ionization energies (I_d) and electron affinity (A_a) of donor and acceptor molecules $I_d - A_a$, the above classification of molecular complexes is fulfilled. For weak CCTs, which are mainly considered here, the energy W_1 of the state of the polar component D^+A^- exceeds the energy W_0 of the non-polar state DA, i.e. $W_1 >> W_0$ [91]. Polar states can be populated during photoexcitation as a result of optical transition with charge transfer.

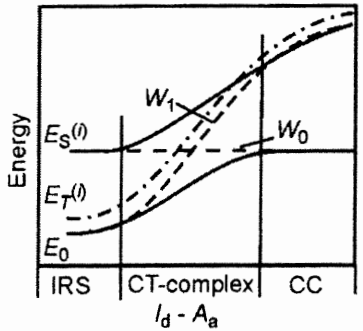

Fig. 1.8. Energy diagram of various types of D-A complexes [99]

Since the photoconductive information media containing molecular complexes are solid solutions of these molecules in the polymer matrix, the need for their plasticization determines another important feature of the studied media – a low concentration of dopant molecules (less than 5 %) which excludes their interaction. Thus, films with D-A complexes as molecular solids are characterized by strong intramolecular interaction (~ 1 eV) and weak interaction between the molecules of the complex ($10^{-3} - 4 \cdot 10^{-2}$ eV). Therefore, the molecules retain their individuality, the energy structure changes slightly (~ 0.2 eV), and the optical and electrical properties of a solid are determined by the

properties of the molecules and their complexes. Optical absorption is molecular and its spectrum is caused by the energy structure of the molecules of a complex [111].

Fig. 1.9 shows the energy of the Van der Waals interaction of the ground state (curve I) and the excited states curves (II, III), where E_0 (curve I) is the ground state energy S_0; $E_S^{(1)}$ (curve II) and $E_S^{(2)}$ are the energies of the 1st and 2nd excited states S_1 and S_2; E_{ex} (curve III) is the energy of the exciplex state; r_0^E, r_0, r_{ex} are the distance of charge transfer in the complex: r_0^E – before the relaxation of the vibrational energy, r_0 – after the relaxation, r_{ex} – after the formation of an exciplex. W_{DA}^0 and W_{DA}^E are the D-A interaction energies in the ground ($\delta = \delta_0 \rightarrow 0$) and excited ($\delta \rightarrow 1$) states. The energies R_E and R_N characterize the contribution of the D – A interactions in the excited and ground states, and their difference $R_E - R_N$ is the change in the D-A interaction energy during photoexcitation $\Delta W_{DA} = W_{DA}^E - W_{DA}^0 \approx 1$ eV (Fig. 1.9). This change exceeds the intermolecular interaction energy by more than 2 orders of magnitude which ensures a weak interaction of the CCT molecules in a solid.

The redistribution of electron density during the complex formation results in the appearance in the absorption spectrum of new bands associated with charge transfer.

Their energies are determined by the following relationship:

$$h\nu_{CT} = E_S^{(i)} - E_0 = I_d - A_a + R_E - E_0 - E_C + R_N, \qquad (1.4)$$

where E_0 and $E_S^{(i)}$ are the energies of the ground and excited (i-th) state of CCT; R_E is the destabilization energy of the excited complex appeared due to the exchange-polarization (resonance) interaction; R_N is the charge transfer energy, stabilizing complex; E_C is the Coulomb energy stabilizing complex in the excited states and described by curves II and III in Fig. 1.9.

The weak intermolecular interaction in a molecular solid [111, 112] leads to a significant localization of charge carriers on individual molecules (localization time $\tau_{loc} = 10^{-12}$–10^{-14} s). This causes electron polarization of the lattice by the charge carrier (the polarization time $\tau_{pol} = 10^{-16}$–10^{-15} s). The time of carrier transfer between neighboring localized states, i.e. jump time $\tau_{hop} = 10^{-12}$ s. As a result, $\tau_{hop} > \tau_{loc} > \tau_{pol}$ and carrier transfer are described by incoherent jumps between localized states. The transition rate (Γ_{ij}) between two hop centers with a distance r_{ij} and the electron binding energy difference $\Delta_{ij}E$ within

the framework of the phenomenological model of hopping mobility can be described by the following relation:

$$\Gamma_{ij} = \Gamma_0 \exp[-2\gamma r_{ij} - (\Delta_{ij}E/k_BT)\Theta(\Delta_{ij}E)], \qquad (1.5)$$

where γ is the attenuation constant of the wave function of a localized electron, which is assumed to be spherically symmetric; $\Theta(x)$ is a single Heaviside step function. For a given spatial distribution of the hopping centers and the type of distribution of the binding energies, we arrive at the problem of random walks of a charge carrier on a spatial lattice of nonenergy centers known as the r-E – percolation problem. The stage of the transfer, as well as the processes of absorption of photons by the molecules of the complexes, are usually described by introducing the concept of charge-transfer state (CT-states) -excited neutral states of the complexes (Fig. 1.10).

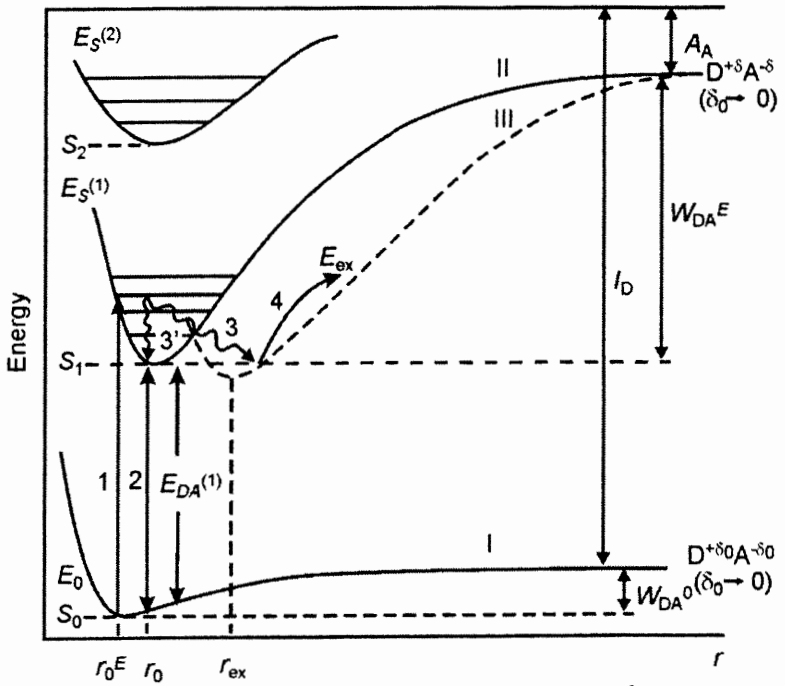

Fig. 1.9. Energy diagram of various D-A complexes for the different distance between molecules r

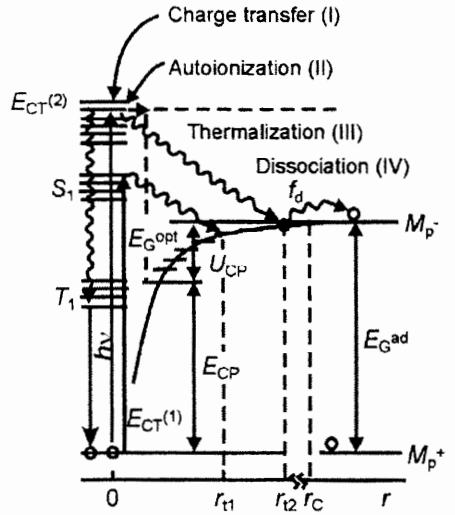

Fig. 1.10. Energy diagrams of the main stages of the photogeneration process in molecular crystals of the polyacene type

In Fig. 1.10 E_G^{opt} and E_G^{ad} are the optical and adiabatic energy gaps; M_p^+, M_p^- are the conductivity levels of molecular polarons; S_1 and T_1 are the singlet and triplet states of the molecule; r_{t1} and r_{t2} are the radii of thermalization of two possible states of relaxed bounded charge pairs (CPs) with energies E_{CP} and U_{CP}; $E_{CT}^{(1)}$ and $E_{CT}^{(2)}$ are the energies of the CT-states, r_C is the Coulomb radius of the bounded pair, f_d is the probability of dissociation. In the ST-states, unlike excitons, where an electron and a hole are localized on a single molecule with a time-independent distance between them, the excited electron moves to the molecule nearest or next to it, but remains Coulomb linked to its hole. The $E_{CT}^{(i)}$ and E_{CP} energies of these nonconducting ionic states lie below the conduction band (Fig. 1.10). When a photon is absorbed by a molecule of solid, either autoionization occurs (Frank-Condon transition from the ground state to one of the excited ones) or direct excitation of the CT-state [112, 113] followed by the formation of a Coulomb bonded charge state (CP-state), as a result of which free charge carriers can appear (Fig. 1.10).

Thus, the peculiarities of molecular media are associated with weak intermolecular interaction in them resulting in, firstly, the molecular nature of light absorption and the subsequent

photogeneration of charge carriers through the state of a Coulomb bounded pair with a quantum yield less than 1 and, secondly, to the localization of charge carriers and their low mobility compared to semiconductors. In semiconductor materials, carrier mobility μ is not less than 1 $cm^2/(V \cdot s)$. Weak intermolecular interaction and strong localization of charge carriers on individual molecules in a molecular solid cause the photogeneration of charge carriers through the state of a Coulomb bounded pair formed by molecular absorption of a photon with possible direct excitation of CT-states. Organic semiconductors are characterized by weak intermolecular interactions of the Van der Waals type, and, for example, in the case of a molecular crystal, a photon is absorbed by a single molecule, and not by a crystal. In this case, an electronic transition can occur between the corresponding energy levels of the molecule with the formation of not free charge carriers, but neutral molecular excitations capable to move through the crystal. Such excitations are called molecular excitons or Frenkel excitons [110–117]. Frenkel exciton is considered as a strongly bounded system of the excited state of a single molecule. On the other hand, there is a well-known model of Wannier-Mott excitons, a weakly bound electron-hole pair with a small value of the Coulomb interaction [40] (Fig. 1.11).

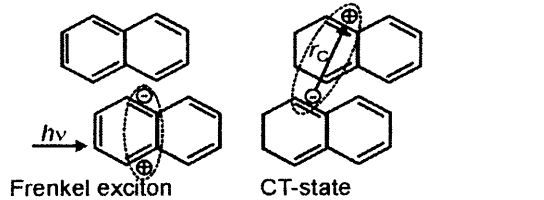

Fig. 1.11. Schematic presentation of the Frenkel exciton (*a*) and the CT-state (*b*) arising in an organic semiconductor upon photoexcitation

Photogeneration of charge carriers in media with weak intermolecular interactions occurs through the state of a Coulomb bounded pair of carriers with the opposite sign. The process of separation of such a pair of charges in an external electric field E includes two stages: the stage of thermalization of the charge carrier connected in the

pair and the stage of the thermal field dissociation of the connected pair of charges [101]. At the first stage, the bounded charge carrier (electron) loses the excess of kinetic energy received from the photon and comes into equilibrium with the phonons at some distance between the charges called the thermalization radius r_t. This stage is characterized by the quantum yield of the formation of bounded pairs η_0. The stage of the thermal field dissociation consists in the separation of thermalized bounded pairs facilitated by an external electric field due to interaction with phonons, and is described by the dissociation probability $f_d(rt, \theta, E)$. In this case

$$\eta = \eta_0 \cdot f_d(r_t, \theta, E) \cdot g(r, \theta) \cdot dr^3, \qquad (1.6)$$

where $g(r,\theta)$ is the distribution function of pairs by the magnitude of the radii r and their orientation respectively to the direction of the field E, θ is the angle between the vectors **r** and **E**. When $r_t < 10$ nm, $g(r,\theta) = \delta(r - r_t)$ and expression (6) is transformed into following:

$$\eta = \eta_0 \cdot f_d(r_t, E). \qquad (1.7)$$

Since at the second stage the process of separation of a carrier pair in the field E has a diffusion-drift character, in the general case it can be described by the three-dimensional Smoluchowski equation. It allows determining the space-time probability density equal to the probability of mutual thermal field dissociation of the Coulomb bonded charges $f_d(r_t,E)$ with a time-independent constant microscopic mobility. In the stationary case of an isotropic system of non-interacting charge pairs that are in equilibrium with a medium with a constant dielectric constant ε and at a constant T, the probability of dissociation $f_d(r_t,E)$ of a pair of charges being at a distance r_t from each other (r_t does not depend on E, T, and photon energy) is determined by the three-dimensional Onsager model:

$$f_d = (1 - k_B T/eE_f r_t) \sum_j (eE_f r_C/k_B T) I_j(e^2/\varepsilon r_t k_B T), \qquad (1.8)$$

where $Ij(x) = I_{j-1}(x) - x_j/j!$ .exp(x), $j > 1$, $I_0(x) = 1 - \exp(-x)$. At constant E and T, expression (8) can be brought to the followed form:

$$f_d(r_t, E) \sim \exp(1 - \exp(r_t/r_c)). \qquad (1.9)$$

To eliminate the limitations of the classical Onsager model, a number of its modifications were proposed: 1) one-dimensional model [119] for description processes in linear systems, 2) "ballistic" model [120] took into account the drift of the bonded carrier during

thermalization (for $r_t > 5$ nm), 3) non-stationary model of photogeneration describing the kinetics of the $f_d(r_t,E)$ probability with $t < 10^{-8}$ s, 4) the Mozumder model [121, 122] giving the dependence of $f_d(r_t,E)$ on the concentration of bonded pairs, 5) the optical model Bessler [101,109]. For anisotropic media, the more general than the Onsagerian model of the Scher-Rakovsky [123], Riesa [124], outgoing from the hopping nature of the separation of charge carriers in a pair and operating by the calculated Monte-Carlo methods of the probabilities of this process are proposed. These models allow us to determine the range of applicability of the Onsager isotropic model and show that the latter is valid for $r_t > 1$ nm, $T > 200$ K.

The probability $f_d(E)$ can also be calculated using the Poole–Fraenkel model [95, 96] which describes the probability of release from the Coulomb center of a mobile charge carrier (with mobility > 1 $cm^2/(V \cdot s)$) under the assumption that the external the electric field E affects the activation energy of this process and lowers the height of the barrier to be overcome by $\sim E^{1/2}$. However, this model and its modifications require the applicability of a band model which is impossible for molecular semiconductors. It should be noted that among the mathematical models considered above describing the process of photogeneration through the state of a Coulomb-coupled pair, the Onsager model most accurately reflects the physics of the process for thermalized pairs. However, since it does not describe the initial stage of the process, it does not allow to take into account the presence of photoexcitation and the influence of the D-A interaction at the thermalization stage and to find the dependences of η on the photon energy and the structure of the photogeneration center molecules.

All physical models of photogeneration differ in the processes leading to the separation of pairs at the distance r_t. In various jump models, such a process is a carrier jump from an excited molecule of the complex to a neighboring intermediate state. In the dissociation-hopping model, these are jumps over localized states with dissociation according to the Poole-Fraenkel model [95, 96]. Dissociation models of the Onsager photogeneration differ in the pre-dissociation stages depending on the structure of the medium, i.e. nature of energy relaxation after photoexcitation. For example, for polyacene crystals in the near-threshold absorption region, with an increasing number of aromatic rings, η increases from 10^{-3} to 0.5. The

photogeneration process in molecular crystals occurs through the CT-states formed when a photon is absorbed (Fig. 1.10, transition (I)) due to excess of the vibrational energy of about 0.3 – 0.4 eV. This energy is lost (Fig. 1.10, transition (III)) for the interaction with lattice phonons after 80–100 collisions at a distance $r_t \sim 6$–10 nm. This process does not depend on the field strength E.

The resulting state of a bounded pair with radius r_t (CP-state) absorbing additional energy from the environment can form free charge carriers (Fig. 1.10, transition (IV)). In the considered model, η and r_t depend on the photon energy [91, 121]. At high energies, the process of autoionization (II) can occur. However, for widely known poly-N-vinylcarbazole (PVC) [95] it was shown that in the region of singlet absorption bands, the quantum yield of photogeneration η increases stepwise with increasing radiation energy hν but in each band η and r_t are stable. The mechanism of photogeneration of charge carriers in FPC near the intrinsic absorption edge can be described by the model proposed for molecular crystals which, like polymers, are characterized by weak intermolecular interactions. It has been shown for them that within the near-threshold region, the spectral dependence of the quantum yield is:

$$\eta(h\nu, T, E) \sim A(E, T)(h\nu - E_G^{ad})^{2/5}, \qquad (1.10)$$

where A (E, T) is a function of temperature T and the electric field strength E. The difference between E_G^{ad} and E_G^{opt}, determined by the energy intervals between the conduction levels of the excited relaxed (CP-charge pair) and unrelaxed (CT-charge transfer) states, is within the range of 0.1 – 0.25 eV and is equal to the formation energy of the molecular polaron E_p participating in the process of photogeneration of charge carriers through CP-states (Fig. 1.10).

In molecular media, this process is multistage, and it is described by the so-called autoionization model of its own photogeneration. According to this model, the formation of CP-states caused by the thermal field dissociation resulting in the appearance of free carriers occurs in several intermediate stages (Fig. 1.10): 1) photogeneration of the neutral exciton state (formation of CT-states) (stage (I)), 2) autoionization of the exciton state, resulting in the formation of a positive ion and a quasi-free electron (stage (II)), 3) thermalization of the "hot" electron due to inelastic scattering on lattice vibrations leading to the formation of a thermalized CP-state (stage (III)). At the final

stage, as a result of thermal dissociation (stage (IV)) under the action of the Coulomb and external fields, according to the Onsager theory, the formation of free charge carriers occur. They become free at a distance of the Coulomb radius $r_C \approx 15–20$ nm [93] which is determined by the equality of the Coulomb and thermal energies.

For molecular media based on donor-acceptor complexes, along with hopping and dissociation-hopping models, an exciplex model can be distinguished for the structural-chemical sensitization of the photoelectric effect and the radical ion model [75, 125] with spectral sensitization with dyes. According to the exciplex model, photogeneration occurs as a result of the thermal field dissociation of the unrelaxed state of the exciplex (curve III in Fig. 1.10) formed during the absorption of a photon by a donor molecule or an acceptor molecule which are the intramolecular CCT (curve II). Then the electron is thermalized. Within this model, the radius is $r_t = 2–3$ nm and may be independent of E and hv in the absorption band due to fast intramolecular relaxation (transition 3′) of the molecule absorbed the photon.

For the spectral sensitization of the photoelectric effect, the photogeneration process is carried out from the states of the bounded ^{1,3}[IRP] radical ion pair, arising from the exciplex state of the molecule absorbing the photon and the molecules from the transport zone. The ^{1,3}[IRP] state dissociates into free carriers and, moreover, as a result of a singlet-triplet conversion with a constant k_{st} depending on the intensity of the magnetic field can become ^{3,1}[IRP] [126–131].

One of the most promising for practical applications is the FPC sensitized with organic, in particular, polymethine and merocyanine dyes, the class of which is very extensive, and the structure is easily variable. These dyes are used as sensitizers of photoconductivity of photoconductive polymers due to their ability to efficiently transform light energy, intense absorption bands within a wide spectral range, the possibility of flexible variation in extremely wide limits of their spectral and other photophysical properties with a change in chemical structure. These dyes are used as sensitizers of photoconductivity of photoconductive polymers due to their ability to efficiently transform light energy, intense absorption bands within a wide spectral range, the possibility of flexible variation of their spectral and other photophysical properties with changing the chemical structure. They are convenient for

modeling the dependencies of the photoelectric properties of FPC versus the molecular structure. These dyes can be used in media for electroluminescent devices, photoelectric converters, holographic recording [132–134].

For widely used information media based on various carbazolyl-containing polymers and oligomers such as, for example, oligo-N-epoxypropylcarbazole (PEPC) high values of photoconductivity were obtained. Therefore, in view of the prospects of such systems, it is important to consider the features of the photogeneration processes in FPCs based on polymers and oligomers of the carbazol-containing type doped with organic dyes as sensitizers of photoconductivity. The linearity of the graphs of dependencies of the photocurrent on the electric field in the coordinates $\lg j_{PH}$ from $E^{1/2}$, the nearness of the value of the coefficient β in (1.3) to the theoretical value of the Poole–Frenkel constant [95, 96], the possibility to use the expression (1.3) for a description of the dependencies of j_{PH} on E for many of these systems allow the use of previously developed models of photogeneration and transport of charge carriers in films of carbazolyl-containing polymers [64, 95, 101].

According to these model concepts, the photogeneration of charges from photogeneration centers, which are dopant molecules (dyes and related compounds), proceeds in two stages. At the first stage of photogeneration, after absorption of a light quantum by a molecule of a dye or similar sensitizer, a bounded EHP is formed. The EHP contains a hole to which corresponds the radical cation (Cz^+) of the carbazolyl fragment (Cz) of the polymer, and an electron remaining in the sensitizer molecule after the hole has left. In the simplified forms, the unexcited molecules of the investigated sensitizers and sensitizers that capture the electron from the carbazolyl unit can be represented as Dye and Dye^-. This allows us to present the process of the formation of EHP in films of carbazolyl-containing polymers with dyes or related compounds (sensitizers) by the corresponding reactions with electron transfer:

$$Cz + Dye \rightarrow Cz^+ + Dye^- \qquad (1.11)$$

At the second stage of photogeneration, a hole from the carbazolyl unit of the Cz^+ polymer either recombines with an electron in the same dye molecule in which it was born (geminal recombination according to scheme (1.12)), or removes from the electron by

transitions between neighboring Cz (dissociation of the EDP according to (1.13)):

$$Cz + ... + Cz + Cz^+ + Dye^- \rightarrow Cz + ... + Cz + Cz + Dye + h\nu_r \quad (1.12)$$

$$Cz + ... + Cz + Cz^+ + Dye^- \rightarrow Cz + ... + Cz^+ + Cz + Dye^- \rightarrow$$
$$\rightarrow Cz^+ + ... + Cz + Cz + Dye^- \quad (1.13)$$

When charges recombine in accordance with the scheme (1.12), the valence electron from the radical form of the dye or another sensitizer Dye^- transfers to Cz^+. After the relaxation of the excited state with radiative release of $h\nu_r$ energy or nonradiative heat release, this dye molecule can again absorb a light quantum and participate in the photogeneration of the EHP. As a result of the dissociation of the EHP according to the scheme (1.13), the electrostatic interaction of a hole with an electron localized in Dye^- relaxes.

The probability of dissociation of EHP increases with increasing E and T in accordance with (1.3). If we take into account the finiteness of the time interval between the moment of absorption of a light quantum at the absorption center and the moment of formation of the EHP, we can assume that between these two points in time there must be a state including a molecule excited by the light and at least one unexcited molecule from the transport zone to which the charge will be transferred. Such short-lived states can sometimes be traced at the level of individual molecules. They are investigated using various techniques including optical detection and tunneling spectroscopy [135–151].

The exciplex state [152] can be attributed to the intermediate state between the act of light absorption and the formation of an EHP. Exciplexes are considered as metastable centers of carrier photogeneration. Photogeneration of charge carriers through the formation of exciplex states was investigated [153, 154] in PEPC films using the example of the dye Rhodamine 6G (R6G). Such a state is detected by the absorption spectrum of the exciplex and by the induced photoconductivity of PEPC films with R6G within the absorption range of the exciplex at the edge of the R6Z absorption band near $\lambda = 590$ nm. At room temperature, it conserves more than one second after the cessation of irradiation of films with light from the region of absorption of R6G near $\lambda = 540$ nm [153, 154]. Exciplexes are formed by excitation of dye molecules and the appearance of specific CCTs between them and carbazole fragments of PEPC. Their formation is confirmed by the appearance of a new

fluorescence band with a maximum at a wavelength $\lambda = 590$ nm occurring under annihilating exciplexes and is absent in the spectra of other polymer films with P6G where exciplexes are not formed.

Since the ground exciplex state is similar to the CCT state, for the formation of free charge carriers, an exciplex transition from the ground state to an excited one is necessary when the light quantum of is absorbed from the absorption range of the exciplex. In this case, the complete transition of an electron from a donor to an acceptor is carried out and then the formation of an EHP is possible, the thermal dissociation of which in an external electric field will lead to the formation of free carriers. Thus, the photogeneration of free current carriers occurs by a two-quantum mechanism revealing itself in PEPC films with R6G in enhancing their photoconductivity upon additional irradiation with light from the absorption range of exciplexes. However, the lifetime of the exciplex state, from which the photogeneration of current carriers occurs, is more than 6 orders of magnitude greater than that estimated at [155] by the attenuation of R6G fluorescence in 2,5-bis-(p-diethylaminophenyl)-1,3,4-oxydiazole. In this compound, is also assumed that the formation of exciplexes and free charge carriers is a result of the dissociation of the EHP.

Such a huge difference in the lifetimes of exciplex states is connected with the difference in the spin states of photogenerated exciplexes and EHPs in different polymer matrices. They are detected by a photoinduced EPR signal of illuminated films which include the radical cation of carbazole Cz^+ [154]. In this case, the kinetics of relaxation of the triplet exciplex state corresponds to a simple exponentially decreasing dependency and confirms the two-molecular composition of the exciplex state. However, for PEPC films with R6G, as for other FPCs, within the visible light range, the linear dependence of j_{PH} on the intensity of the absorbed light is observed. It is not quadratic. This means that the exciplex mechanism of formation of free charge carriers is not the main. EHPs are formed as a result of the excitation of the photogeneration center, the relaxation of the photogeneration center to the lower excited state, and the ionization of the photogeneration center from the lower excited state as a result of the intermolecular electronic transition.

In this scheme, the probability Φ_0 of photogeneration of an EHP, the formation of singlet or triplet spin states of charge carriers in an

EHP is determined by the ratio of the probabilities of the radiative and non-radiative relaxation channels of the excited state (intramolecular conversion and interconversion) of the photogeneration center dissociation of EDP [156–160].

Often [64, 161–166], in molecules of organic dyes and related compounds, the lower excited triplet state has less energy than the lower excited singlet state, and the allowed transitions between states S_1 and S_0 are radiative, and the transitions between T_1^0 and S_0 are nonradiative. To explain the interdependence of the conversion and photogeneration processes, we use the scheme in Fig. 1.12.

In Fig. 1.12 P is the efficiency of photoexcitation of molecules from the ground singlet state (S_0) to the excited unrelaxed singlet (S_1^u) state of the photogeneration center; N_1, N_3 are the concentrations of photogeneration center molecules in the lower relaxed singlet (S_1^0) and triplet (T_1^0) excited states respectively; n_1, n_3 are the EHP concentrations in the singlet (S) and three triplet states (T_0, T_-, T_+) respectively [167, 168]; k_u is the velocity constant of the internal conversion S_1^u–S_0; k_{Su} and k_S are the velocity constants of the radiationless and radiative transition S_1^0–S_0; k_T is the transition velocity constant for T_1–S_0; k_2, k_{-2} are the velocity constants of intramolecular interconversion S_1–T_1 and T_1–S_1; k_1, k_{-1} are the velocity constants for the formation and recombination of singlet EHPs; k_3, k_{-3} are the velocity constants for the formation and recombination of triplet EHPs; k_{ST} is the velocity constant of spin conversion of EHP; k_η is the velocity constant for the dissociation of the EHP into a free electron (e^-) and a hole (p^+).

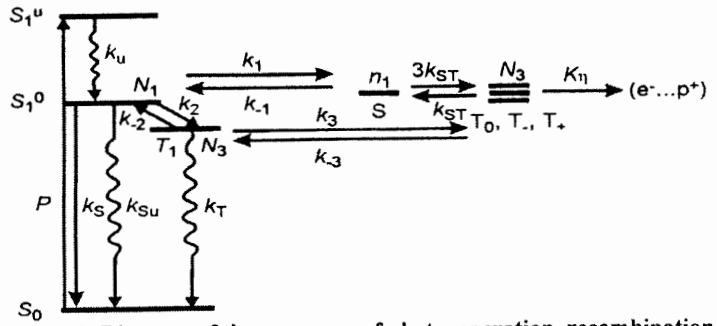

Fig. 1.12. Diagram of the processes of photogeneration, recombination and dissociation of charges in the EHP

In some cases, this scheme is sufficient to describe the experimentally observed dependences of Φ_0 and η on the structure and concentration of molecules of photogeneration centers forming the corresponding transport zones, as well as on E, T, and λ. From the diagram in Fig. 1.12 it follows that with the usual ratio $k_{-1} > k_{-3}$, the quantum yield of the photogeneration of charge carriers increases with an increase in the fraction of triplet EHPs respectively to the fraction of singlet EHPs. For this, it is desirable to fulfill the following conditions:

$$k_2 > k_{-2};\ k_1 > k_S;\ k_3 > k_T;\ k_\eta > k_{-1}, k_{-3}. \qquad (1.14)$$

Condition (1.14) is fulfilled: with an increase in the structural rigidity of the molecules [151]; in physical dimers and aggregates of dyes [163, 164] when there is a rather strong overlap of the S- and T-states [165–169]; upon using magnetically active ions ion dyes [170, 171] when an unpainted counterion affects the S-T conversion of EHP. Besides, in strong electric fields, the possibility of thermal field ionization of photogeneration centers from excited states with a short lifetime is not excluded when k_1 and Φ_0 increase. For example, in FPC based on PEPC with CCT, the increase of photoconductivity in strong electric fields correlates with the quenching effect of the field on the photoluminescence intensity, and the photoluminescence quenching does not depend on temperature within the range $77 < T < 230$ K and has an activation energy ~ 0.1 eV for $T > 280$ K [171].

The action of an external electric field here is not only in lowering and increasing the transparency of the potential barrier for the carrier to exit the photogeneration center, but also promotes the redistribution of electron density inside the molecules in the direction of this barrier, and induces an electric charge of the opposite sign in the molecule to which the electronic transition occurs. The probability of dissociation of EHP increases not only with an increase in the lifetime of the EHP but also with an increase of k_η. The latter is reached in accordance with (1.3) with increasing E and T, as well as by increasing the concentrations of N_a and N_d with a strong delocalization of the corresponding boundary molecular orbitals. Here the effect is not only that under such conditions intermolecular electronic transitions are facilitated. First, the carriers of both signs leave the photogeneration center, which is also a recombination center, and the probability of their geminal recombination decreases sharply. Secondly, with an increase

in the delocalization of electric charges in an EHP, the energy of electrostatic interaction between them decreases and, as a result, the W_{0PH} in (1.3) decreases. That is why, apparently, high photoconductivity of FPC is observed in branched polymers or monomers, as well as in FPC based on porphyrins, fullerenes, and graphene when steric factors impeding intermolecular electron transfer are reduced to a minimum [172–179].

To achieve high photoconductivity, FPC should possess maximum spatial separation of charge carriers in an EHP and their triplet spin state reducing the probability of recombination. Recombination is a competing process respectively to the formation of free charge carriers. The presence or absence of a potential barrier for the carrier transfer from the molecule (part of the transport zone (Fig. 1.1)) to the recombination center, which in the case of geminal recombination was also the center of photogeneration, is considered to be determining. Examples of photoconductive FPCs and their use in information media are presented in subsequent chapters.

1.4. Spin-dependent effects in the photogeneration mechanism

The high photoconductivity of the FPC is primarily ensured by the efficiency of the formation of the EHP from excited states of the photogeneration centers (Fig. 1.1). Since the spin state of the EHP and the excited photogeneration center are the same at the initial stage of EHP formation, it can be assumed that the quantum yield of photogeneration of free charge carriers is directly proportional to the quantum yield of EHP formation, and $\eta \sim \eta_0$ in (1.3). However, this is not always the case. The fact is that the EHP contains not just electric charges but radical ions of the organic structures making up the FPC. Unpaired electrons in the ion-radical interact with other electrons and nuclei [165–169]. The latter changes the initial spin state of the EHP (Fig. 1.12) as a result of intercombination conversion (S-T-conversion).

Besides, unpaired electrons and nuclei can also interact with an external magnetic field, which can be created in an experiment, or exist in FPC in a local region near a high-spin 3rd particle. This opens up an additional opportunity to study the initial spin state of the EHP and the mechanisms of its transformation until geminal recombination or dissociation. Often, such studies are based on the observation of changes in the intensity and kinetics of fluorescence or photoconductivity of FPC before and after switching on an external magnetic field [180]. In this case, one can use simple characteristics of the spin state of an EHP. According to the process diagram in Fig. 1.12 magnetic field makes S-T-conversion difficult. Therefore, for singlet EHPs, the magnetic field should increase the probability of geminal recombination, which means that recombination luminescence is flared up in a magnetic field, and the photoconductivity decreases.

For triplet EHPs, the opposite is true: in a magnetic field, recombination luminescence is quenched, and photoconductivity increases. Since fluorescence is not always observed at room temperature, in these cases methods of measuring the density of the photocurrent j_{PH} are used before and after switching on the magnetic field H. The influence of the magnetic field is estimated by the value $\delta j_{PH} = (j_{PH}(H) - j_{PH}(0))/j_{PH}(0)$, where $j_{PH}(0)$ is the photocurrent density before turning on the magnetic field, $j_{PH}(H)$ is the photocurrent density after switching on the magnetic field H. Let us consider several previously presented examples of obtaining information on the spin state of an EHP in the FPC.

The effect of H on the photoconductivity of FPC, in which the CCT is the center of photogeneration, was studied [181] using the example of PEPC oligomer films doped with the acceptor 2,4,7-trinitro-9-fluorenone (TNF).

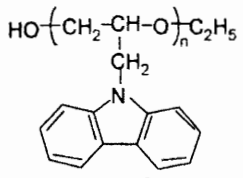

PEPC

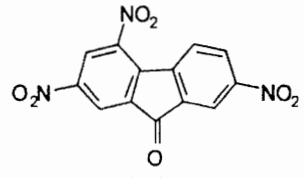

TNF

The samples were investigated in the form of a sandwich-structure (glass substrate – ITO – PEPC film + N wt. % TNF – Al), where N is the concentration of TNF. It was found that at constant E and T within the range of $H \leq 5$ kOe, the magnetic field reduces j_{PH}. The change in j_{PH} does not depend on the orientation of the sample relative to the direction of the magnetic field lines. The results of measurements at room temperature [181] are shown in Fig. 1.13.

Since the influence of H leads to a decrease in the photocurrent, this effect is considered [181] as negative. The dependencies of δj_{PH} on H saturate at $H \leq 1$ kOe, the dependences of δj_{PH} on E for various N are almost parallel and, with increasing N, shift to the region of large $|\delta j_{PH}|$ and with increasing E $|\delta j_{PH}|$ are decreasing. Dependency $|\delta j_{PH}|$ on E, and also independency on E (within the range of $E \leq 1 \cdot 10^8$ V/m) of the photogeneration activation energy W_{0ph} in (1.3) possessing physical meaning as the binding energy of charges in the EHP at a distance between charges r_0 allow to count that effect of H on η happens at the second stage of photogeneration i.e. at the stage of dissociation of EHP.

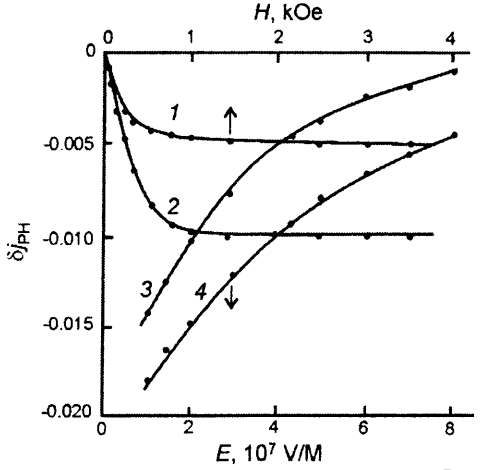

Fig. 1.13. Dependencies δj_{PH} on H (1, 2) at $E = 4 \cdot 10^7$ V/m and δj_{PH} on E (3, 4) at H = 3.5 kOe for N = 1 wt.% (1, 3) and N = 4.5 wt.% (2, 4). Excitation light wavelength $\lambda = 633$ nm

The range of the magnetic field strength $H \leq 1$ kOe where j_{PH} is dependent on H [168] indicates that for the considered case the influence of the magnetic field reveals itself within the framework of the hyperfine interaction mechanism of the change in the multiplicity of EHP. This mechanism reveals itself when the external magnetic field H exceeds the local magnetic field created by magnetic nuclei, and when the distance between the charges in the EHP exceeds the spin-correlation radius r_C closed to the Onsager radius.

In PEPC films with TNF, the thermalization radius r_0 calculated from the value $W_{0ph} = 0.44$ eV [182] is 10 Å and is 3–5 Å less than r_C [183]. Thus, the hyperfine interaction mechanism for the interaction of carrier spins with magnetic fields of magnetic nuclei [168, 169] will not manifest itself immediately but after the distance between the charges in the EHP exceeds r_C. The vector model of EHP spin states from the scheme in Fig. 1.12 is shown in Fig. 1.14, *a*. The manifestation of the hyperfine interaction mechanism for an EHP with distances between the charges $r_0 \geq r_C$ in the absence of a magnetic field is shown in Fig. 1.14, *b*. This figure presents the vector model [168, 169] of carrier spin in an EHP with one magnetic nucleus in a zero magnetic field.

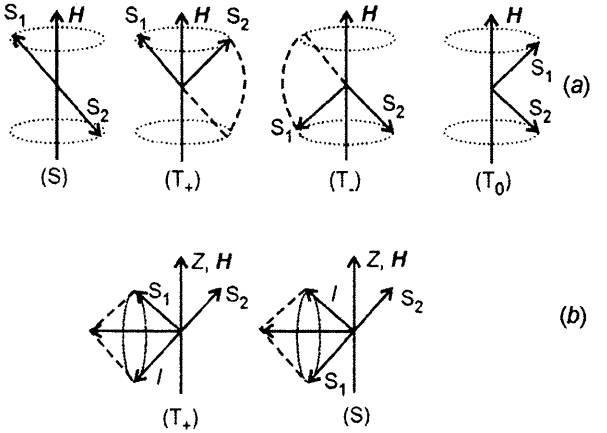

Fig. 1.14. *a* is the vector model of the state of the EHP spins in the singlet (S) and three triplet states (T0, T–, T +) respectively taking into account the presence of a magnetic field. *b* is the vector model of the carrier spin motion in an EHP with one magnetic nucleus in a zero magnetic field

Here, the electronic $\mathbf{S}_1$ and nuclear $\mathbf{I}$ spins of the EHP precess around a common axis. In the course of mutually agreed movement, the spins $\mathbf{S}_1$ and $\mathbf{I}$ perform a mutual turn. The configuration of the EHP spins corresponding to the triplet state (T_+) passes into the configuration of the singlet state (S). The external magnetic field removes the degeneracy from the state of the EHP spins, and for transitions between the (T_0, T_-, T_+) and (S) states additional energy is needed [168, 169]. The external magnetic field imposes a prohibit on transitions between neighboring spin states.

The negative effect of the influence of H on η and j_{PH} indicates that EHPs are formed mainly in the singlet state. When the distance between the charges in the EHP $r = r_C$ is reached, the magnetic field prohibits the transition of the EDP spins from the state (S) to (T_-, T_+). The latter leads to a decrease in the concentration of EHPs with a triplet spin state and, consequently, to a decrease in η and j_{PH}. However, further investigations have shown that in samples with PEPC + N wt.% TNF at $N > 5$ and $E > 5 \cdot 10^7$ V/m, the effect of the influence of a magnetic field changes its sign and becomes positive. This made it possible to assume that both the positive and negative effects of the influence of H on η and j_{PH} are simultaneously present in the dependency of j_{PH} on H. Therefore, the kinetics of the influence of H on δj_{PH} [130] has been studied in more detail.

After H is turned on, the dependency of $|\delta j_{PH}|$ on t increased in the region of negative values, reached the maximum negative value, and then changed in the opposite direction, and after a second turned into saturation. Increase of the dependency of $|\delta j_{PH}|$ on t within the region of negative values occurs during $t \leq 3 \cdot 10^{-2}$ s, and the decrease to saturation occurs during $t \sim 1$ s. Thus, the positive and negative effects of H on η and j_{PH} can be separated in time.

The stationary values of the positive and negative effects do not depend on the orientation of the sandwich-structure sample relative to the direction of the magnetic field lines. The time constant of the rise of the negative effect of the influence of H on η and j_{PH} is less than the time constant of the rise of the magnetic induction of the electromagnet [130]. The time constant of the slow component at T = 293 K is 0.6 ± 0.1 s and does not depend on E, N, and λ (Fig. 1.15) but changed with T and reached a maximum value of 0.9 ± 0.1 s within the range $T = 200 \pm 15$ K.

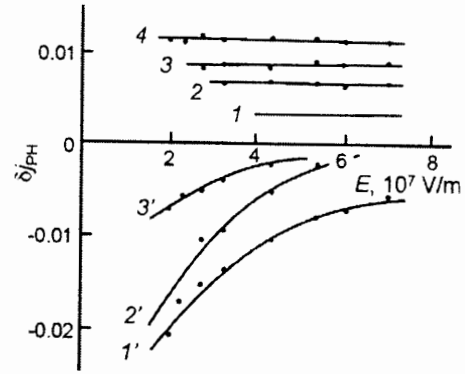

Fig. 1.15. Dependencies of δj_{PH} on E for positive (1–4) and negative (1 '– 3') effects in films PEPC + 4.5 wt.% TNF for H = 1 kOe, λ= 630 nm (1, 1'), 576 nm (2, 2'), 511 nm (3, 3'), 436 nm (4), T = 293 K

Moreover, the values $|\delta j_{PH}|$ of positive effect monotonously increased with increasing H up to the value H = 7 kOe but the time constant of the slow component of the kinetics remained almost unchanged at T = const. Additional studies using NMR found that in solid samples of composites of PEPC with TNF at room temperature and in magnetic fields closed to those discussed in the experiments, the time constant of the spin-lattice relaxation of the magnetic moments of the proton nuclei is $\sim 0.7 \pm 0.1$ s. The latter indicates a possible connection between the slow component of the kinetics of the positive effect with the orientation of the magnetic moments of the molecular components of the CCT after switching on the H.

From Fig. 1.15 it can be seen [130] that the positive effect of H on η and j_{PH} increases slightly with increasing E and decreasing λ, and the negative effect decreases with decreasing λ and is practically not observed at λ = 436 nm. Fig. 1.16 shows the dependencies of δj_{PH} on T, and Fig. 1.17 shows dependencies of δj_{PH} on the number of $-CH_2$ groups on which the molecular mass M in the chain R of R-DDFC acceptor molecules depends. Here, R-DDFC is a derivative of 2,7-dinitro/9digacymethylene /fluorene-4-carboxylic acid. With increasing T, the positive effect decreases, and the negative effect increases. The positive effect does not depend on the acceptor molecular mass M, and the negative effect increases with increasing M and the length of the chain R.

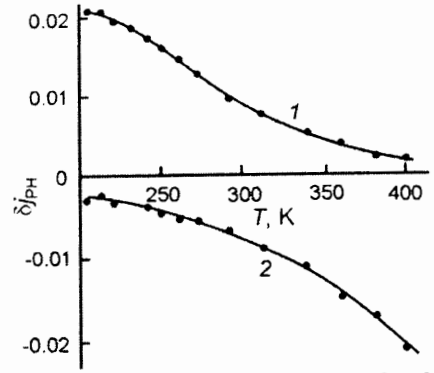

Fig. 1.16. Dependencies of δj_{PH} on T in films PEPC + 0.5 wt. % TNF for λ_{irr} = 460 nm (1) and PEPK + 5 wt. % TNF for λ_{irr} = 680 nm (2) at E = 5 · 10^7 V/m and H = 1 kOe

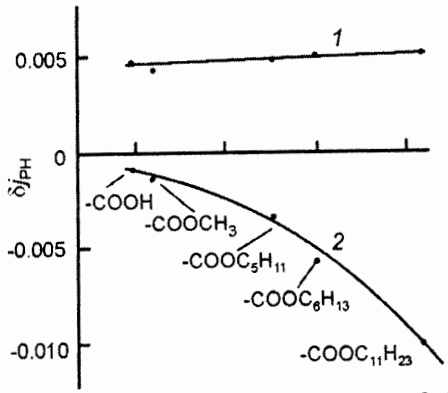

Fig. 1.17. Dependencies of δj_{PH} on the number of -CH_2 groups (molecular weight M) in PEPC + 5 mol. % R-DDFC at λ_{irr} = 460 nm (1) and 680 nm (2), E = 5 · 10^7 V/m, H = 1 kOe, T = 293 K

The weak dependency of the positive effect on E (Fig. 1.15), its dependence on H within the range H > 1 kOe, as well as the large values of the time constant of its increase, suggested [130] that the positive effect mainly reveals itself at the stage of EHP formation. It is assumed that this (first) effect is caused by a change in the orientation of the full magnetic moment of CCT after switching on the magnetic field. This can lead to an increase in the probability of formation of triplet EHPs and, consequently, to an increase in η_0 (see (1.3)).

The growth of the positive effect with increasing E (although this growth is insignificant) and with decreasing λ suggested that the positive effect of H on η consists of two positive effects. The second effect reveals itself at the stage of dissociation of EHP and is caused by the presence of a certain number of triplet EHPs whose concentration increases with decreasing λ. For these EHPs, the distance between the charges is $r < r_C$. An increase in the negative effect with increasing N and its decrease with decreasing λ is caused by the possible formation of triplet EHPs with distances between the charges $r < r_C$. With a decrease of λ excitation of the CCT occurs to higher energy states. When an electron returns to the loofwer excited state from which it is thermalized the probability of electron spin conversion increases. As a result, the formation of an EHP in the triplet state becomes possible. Besides, upon the increase of the distance between the charges in the EHP within the range $r < r_C$ there is an insignificant probability of a change in the EHP multiplicity by the hyperfine interaction mechanism [168, 169]. This probability depends on the time of charge diffusion in the EHP to r_C and grows with its increase.

A grows of N leads to an increase in the electron mobility (see (1)) and, as a consequence, to a decrease of the time of charge diffusion in the EDP to r_C, to a decrease of the probability of a change in the multiplet of the singlet EHP with the formation of triplet EHP. The growth of T leads to the same effect. With its growth, the diffusion velocity of charges in the EHP increases and the time of their movement to r_C decreases. Thus, at distances of charges in EHP $r = r_C$, with increasing N, T, λ_{irr} the concentration of triplet EHP decreases and the concentration of singlet EHP increases. An increase of the concentration of singlet EHPs leads to an increase in $-|\delta j_{PH}|$ due to the prohibition of S-T-transitions in an external magnetic field by the hyperfine interaction mechanism [168, 169].

The peculiarities of the formation and geminal recombination of the EHP with the influence on them of the spin conversion of charges in the EHP were studied [184–186] using the example of an FPC with photogeneration centers CICT1, CICT2, CICT3.

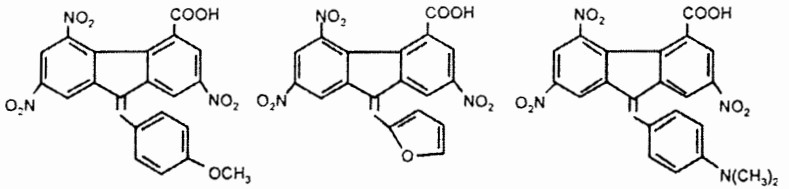

CICT1 CICT2 CICT3

Fig. 1.18 shows the normalized absorption and photoluminescence spectra of PEPC films with CICT1 – CICT3. These spectra do not change within a wide range of concentrations of CICT1 – CICT3 and are identical to the spectra of CICT1 – CICT3 in the electrically neutral polymer matrix of the copolymer of styrene with methacrylate. Later indicates the absence of the formation of a CCT between the carbazole fragments of PEPC and CICT1 – CICT3, and therefore the molecules of CICT1 – CICT3 are the centers of light absorption and photogeneration of charge carriers in PEPC films.

The CICT1 – CICT3 molecules have the same acceptor fragment but different electron-donor groups, as a result, the ionization potentials I_g of these molecules differ [184–186]. The ratio between the I_g of the CICT1 – CICT3 molecules can be estimated from the ratio of the energy of the maxima of the long-wavelength absorption bands $h\nu_{max}$ since I_g and $h\nu_{max}$ are related by the following expression

$$h\nu_{max} = I_g - A_e - U, \qquad (1.15)$$

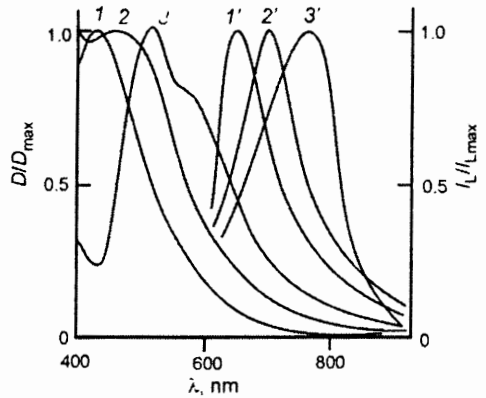

Fig. 1.18. The normalized absorption spectra (1–3) and photoluminescence spectra (1'– 3') of PEPC films with 5 mol.% CICT1 (1, 1'), CICT2 (2, 2'), CICT3 (3, 3')

The values of the electron affinity energy A_e for the considered CICT are the same, and the energy of the electrostatic interaction U between the donor and acceptor parts of the CICT molecules in the excited state are close. Therefore, in the series CICT1 – CICT3, the value of I_g decreases. According to the data in Fig. 1.19, this ratio is 1: 0.94:0.9. This difference in I_g has a significant influence on the efficiency of photogeneration of carriers in FPC based on PEPC with CICT1 – CICT3. In PEPC films with organic acceptors, for example, with TNF forming a CCT with carbazole fragments, the hole mobility is 1.5–2 orders of magnitude higher than the electron mobility [74, 95]. Therefore, in this type of FPC, in the process of photogeneration of an EHP, the hole first leaves the excited CCT and in the initial spatial distribution of the EHP, it is localized on one of the carbazole fragments outside the CCT, and the electron is on the acceptor molecule on the CCT.

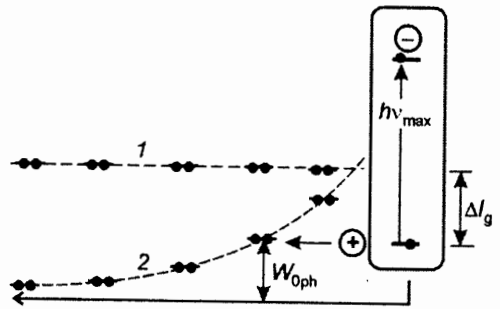

Fig. 1.19. Diagram of the formation and annihilation of EHP in PEPC films with CICT:
1 – HOMO energy of carbazole fragments before the formation of EHP;
2 – after the formation of the EHP

The process of annihilation of EHP, in this case, consists of returning the hole to the ionized CCT to the carbazole fragment which is part of the CCT. In this case, the recombination time constant is ~ 10^{-7}–10^{-6} s. A similar situation of charge recombination in the EHP is also observed in the PEPC films with the investigated CICTs. The difference is that when returning to the recombination center, the hole passes from the carbazole fragment to the donor part of the CICT differing from the carbazole fragment in its electronic structure. This,

apparently, [184–186] determines that the charge recombination time constant in the EHP in PEPC films with the CICT is 8 orders of magnitude longer than the charge recombination time constant in the EHP for PEPC films with TNF. From the measurement results of the dependency of j_{PH} on E and T in samples of PEPC films with SVPZ1 – SVPZ3, it was determined that the activation energy of photogeneration W_{0ph} in (1.3) is 0.41, 0.45, and 0.52 eV respectively, and does not depend on the wavelength of photogeneration excitation light. The thermalization radii r_0 calculated from these values of W_{0ph} are 12, 10.8, and 8.3 Å respectively. Thus, it can be assumed that the EHPs in the studied FPCs are formed as a result of the tunneling transition of a hole from the upper valence level of the donor part of the excited CICT molecule to the upper valence level of the carbazole fragment.

It turns out that the greater the difference in the ionization potential of the CICT molecule and the carbazole fragment (ΔI_g), the greater the r_0 and the smaller W_{0ph}. Considering that the hole tunneling process takes place in the electric field of a quasi-non-moving electron charge, it seems possible to propose the following model of the formation of an EHP (Fig. 1.19). When a CICT molecule is excited and a hole leaves it, the electric field of the electron localized on the acceptor part of the CICT molecule modulates the position of the upper valence levels of the carbazole fragments relative to the upper valence levels of the donor part of the CICT molecule. The levels of carbazole fragments are shifted in the direction of decreasing of W_{0ph}. For some pairs, the carbazole fragment – the donor part of the CICT molecule, the upper valence levels occupy the same energy position, and for them the value $I_g = 0$. The distance between the valence levels in such pairs depends on ΔI_g and increases with increasing ΔI_g. If we assume that the tunneling of a hole during the formation of an EHP occurs between such valence levels, then this explains the difference in the radius of thermalization of the hole r_0 from the CICT1 – CICT3 molecules.

In papers [184–186] one more interesting feature of FPC based on PEPC with CICT1 – CICT3 is noted. It is associated with the photogeneration of the EHP with a long lifetime in these FPCs making it possible to investigate the mechanism of photogeneration by the EPR method. Fig. 1.20 shows the spectrum of the EPR signal

appearing in the PEPC films with the CICT1 – CICT3 when they are irradiated with light from the absorption range of the CICT [184]. The EPR photo signal is characterized by a g-factor g = 2.0023±0.0002 and a width between the points of maximum slope of the absorption curve H_{11} = 9.6±0.3 Oe. EPR spectra have parameters close to the signals of carbazole radical cations.

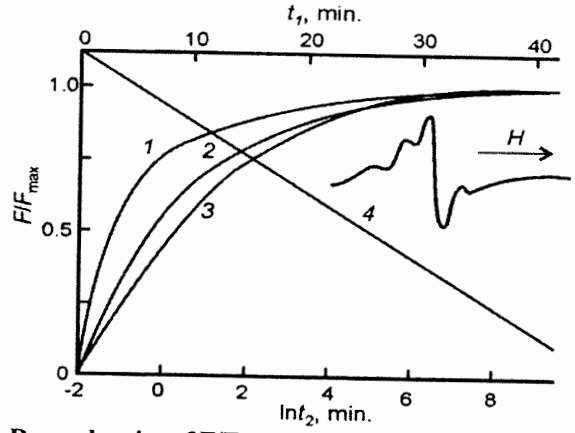

Fig. 1.20. Dependencies of F/F_{max} on t_1 (curves 1–3) and $\ln(F/F_{max})$ on t_2 (curve 4) in films PEPC + 5 wt.% CICT1 (1), PEPC + 5 wt.% CICT2 (2), PEPC + 5 wt.% CICT3 (3). The insert shows the spectrum of the EPR photo signal in films PEPC with CICT1 - CICT3

In Fig. 1.20 curves 1–3 present the results of measuring the intensity (F/F_{max}) of the EPR signal in solid samples of PEPC with 5 wt.% CICT1 – CICT3 on time (t_1) after the start of irradiation with light from the absorption range of CICT, and curve 4 – on time (t_2) after turning off the light. The value F_{max} corresponds to the maximum value of F during prolonged irradiation of the sample with light. The value of F depends linearly on the light intensity, does not depend on the intensity of the external magnetic field within the time interval until the registration of the EPR signal. EPR photo signal with g = 4 was not detected (the g-factor value for paramagnetic particles with the spin number value $m_s = \pm 1$). Besides, no EPR photo signal was detected in specially prepared samples where PEPC was replaced by polystyrene.

It is concluded that the EPR photo signal corresponds to the formation of long-lived EHPs with uncorrelated spins between charges upon irradiation with light and their relaxation after turning off the light. This means that the distance between the charges is greater than the radius of the spin correlation r_C, and the charges in the EHP are quasi-free and paramagnetic. The kinetics of increase of the EPR signal for PEPC films with CICT1 – CICT3 [184–186] are similar but differ by a slower velocity of increase and longer transition times to saturation. However, the dependencies of F/F_{max} on t_2 for films with CICT1 – CICT3 coincide. The larger values of the transition time to saturation and the slower velocity of the rise of the dependency of F/F_{max} on t_1 when CICT1 is replaced by CICT2 and CICT3 are caused by the difference in the thermalization radius r_0. The larger r_0, the smaller the difference $r_C - r_0$ (see Fig. 1.19) and the less time it takes to dissociate the EHP due to the transition of the mobile charge (hole) beyond the spin-correlation radius (according to [187] $r_C \geq 13$ Å).

In the works [184–186], model representations of the formation and annihilation of EHP in FPC based on PEPC with CICT are formulated following from the analysis of experimental results. The formation of an EHP occurs as a result of the tunneling transition of a hole from the upper valence level of the donor part of the excited CICT molecule to the same electronic level of the carbazole fragment. The energy of these electronic levels is the same. In this case, the thermalization radius depends on the difference in the ionization potential of the CICT molecule and the carbazole fragment of PEPC. As a result of hole thermalization, EHPs are formed and their initial distribution can be described by the δ-function. The change in the concentration of EHP occurs due to three reasons. i). Photogeneration of EHP. ii). Annihilation of the EHP during the transition of a hole from a distance r_0 to the recombination center to the donor part of the CICT molecule. This process is described by the time constant τ_a:

$$\tau_a = \nu_1^{-1} \exp(2\, r_0/\alpha_p) \exp(W_p/k_B T), \qquad (1.16)$$

where ν_1 is the frequency factor of tunneling during carrier recombination, W_p is the energy barrier for recombination which is proportional to ΔI_g (Fig. 1.19). The increase in the distance between charge carriers in the EHP as a result of the diffuse movement of holes

inside the carbazole fragments and tunneling between neighboring carbazole fragments. In this case, a new spatial distribution of EHPs is formed. The distance between charges in this EHP distribution is within the range $r_0 \leq r \leq r_C$.

With the time flow after the formation of an EHP as a result of diffusion and tunneling of holes in the direction from the recombination center, a new spatial distribution of the EHP can be formed with the distance between the charges is $r > r_C$. Charge carriers in this spatial distribution already have uncorrelated spins, and they can be detected by the EPR photo signal [181]. This is the spatial distribution of quasi-free paramagnetic particles. The change in the values of the relaxation time constant of the concentration of EHPs of the first spatial distribution at the transition from PEPC films with CICT1 to PEPC films with CICT2 and CICT3 is determined not only by the difference in W_p but also by the values ν_1. For these three FPC with CICT1 – CICT3, from the comparison of the experimental values of W_p, W_{0ph} (and, accordingly, r_0) τ_a can be obtained: $8 \cdot 10^{15}$, $4 \cdot 10^{12}$ and $9 \cdot 10^{9}$ s^{-1}.

According to [187], the frequency factor of charge tunneling at recombination is determined by many conditions, in particular, by the electronic structure and mutual arrangement of the π-electron systems of organic molecules between which tunneling occurs. In the considered case, a difference in the structure of the π-electron systems of the molecules CICT1 – CICT3 actually exists, but it is not so significant for a change of ν_1 in six orders of magnitude. To clarify this apparent contradiction, works [181, 184–186] analyzed the results of investigations of the influence of a magnetic field on the efficiency of photogeneration of current carriers, which are shown in Fig. 1.21–1.23.

It was found [181, 184–186] that in the PEPC films with CICT1, the effect of a magnetic field on j_{PH} is positive (δ_+). It increases with decreasing λ and weakens with increasing E. In the PEPC films with CICT2, both positive and negative (δ_-) effects of H on j_{PH} are observed. These two effects reveal themselves in different ranges of E: δ_+ appears at lower electric field strengths compared to δ_-. With increasing E, the δ_+ effect weakens, becomes zero, and passes into the δ_- effect. With a further increase in E, the effect of δ_- is enhanced. In PEPC films with CICT3 for $\lambda > 400$ nm, only the effect of δ_- is observed, which increases with increasing E and practically does not

depend on λ. Both effects δ_+ and δ_- are fast and do not depend on the mutual orientation of the force lines E and H [184–186]. Fig. 1.21 shows the graphs of the dependency of δj_{PH} on H in the considered FPC. This figure shows that both the δ_+ and δ_- effects are independent of H for H > 1 kOe.

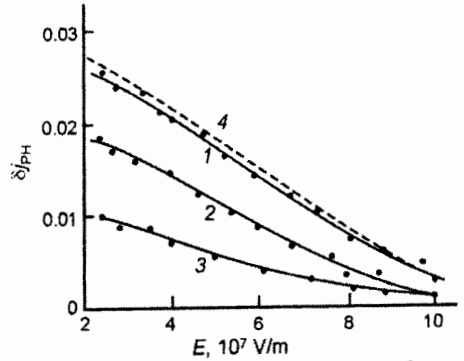

Fig. 1.21. Graphs of the dependency of δj_{PH} on E in films PEPC + 5 wt. % CICT1 for λ = 465 nm (*1*), 580 nm (*2*), 680 nm (*3*) at H = 1 кOe, T = 293 K and (*4*) is calculated by the formula (1.19)

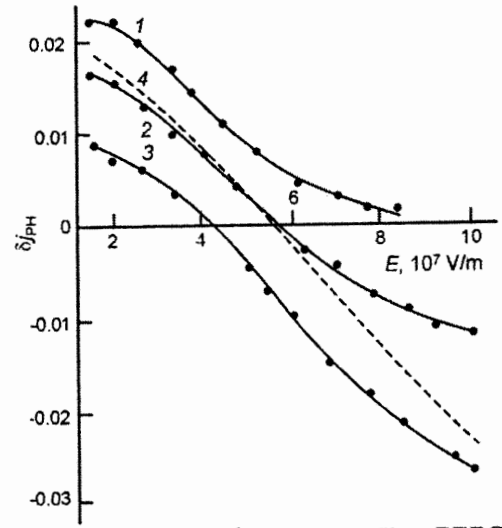

Fig. 1.22. Graphs of dependency δj_{PH} on E in films PEPC + 5 wt. % CICT2 for λ = 465 nm (*1*), 580 nm (*2*), 680 nm (*3*) at H = 1 кOe, T = 293 K and (*4*) is calculated by the formula (1.19)

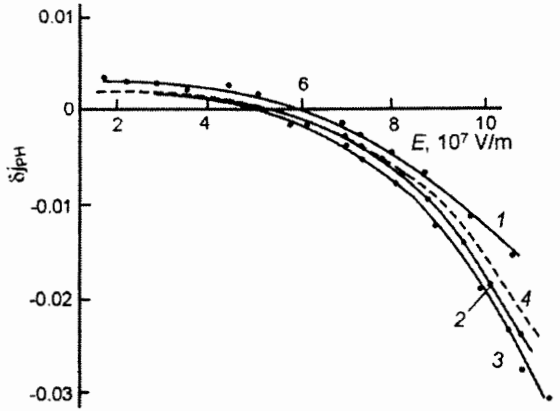

Fig. 1.23. Graphs of dependency of δj_{PH} on E in films PEPC + 5 wt. % CICT3 for λ = 465 nm (*1*), 580 nm (*2*), 680 nm (*3*) at H = 1 кOe, T = 293 K and (*4*) is calculated by the formula (1.19)

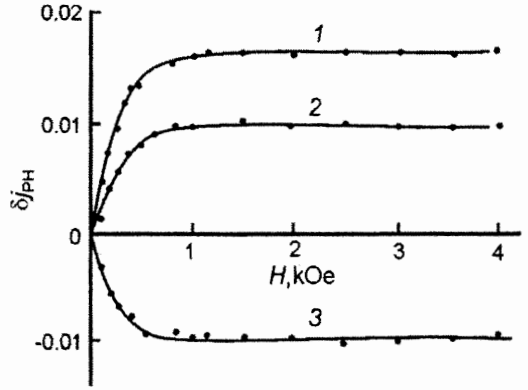

Fig. 1.24. Graphs of the dependency of δj_{PH} on H in PEPC films + 5 wt. % CICT1 (*1*), PEPC + 5 wt. % CICT2 (*2*), PEPC + 5 wt. % CICT3 (*3*) for λ = 580 nm (*2*), E = $3 \cdot 10^7$ V·m^{-1} (*1*, *2*) and $9 \cdot 10^7$ V·m^{-1} (*3*), T = 293 K

The range of the magnetic field strength H ≤ 1 kOe, where the influence of H on δj_{PH} is observed, clearly indicates that the influence of H reveals itself within the framework of the hyperfine interaction mechanism [167, 168]. In this case, H exceeds the intensity of the local

magnetic field of the nuclei and the distance between the charges in the EHP is close to r_C. In accordance with the hyperfine interaction mechanism, the positive effect of H on δj_{PH} and its dependence on E in PEPC films with CICT1 can be explained as follows.

In the absence of external electric and magnetic fields at distances between the charges $r < r_C$, the concentration of triplet EHPs significantly exceeds the concentration of singlet ones. With a further increase in the distance $r \geq r_C$ between the charges in the EHP, as a result of the hyperfine interaction mechanism, a uniform equilibrium distribution of the EHP concentrations over the spin states (T_0, T_-, T_+) and (S) will occur (Fig. 1.14). If the process of increasing the distance between the charges in an EHP occurs in an external magnetic field, then at $r \geq r_C$ in the EHP distribution over spin states, there will be a change in the direction of increasing the concentration of triplet EHPs due to the prohibition on spin conversion, which is overlayed by an external magnetic field [167, 168].

For photogeneration of charge carriers, the triplet state of an EHP is preferable because the lifetime of such EHPs is longer compared with the singlet ones. Therefore, an increase in the concentration of triplet EHPs at $r \geq r_C$ in an external magnetic field leads to an increase in the photogeneration efficiency of charge carriers and a positive effect δ_+. The external electric field allows not only to reveal the effect of δ_+ but it reduces it and almost completely eliminates this effect at $E = 1 \cdot 10^8$ V· m^{-1} (Fig. 1.21). In the considered range of E, the time constant for increasing the efficiency of photogeneration has values that are commensurate and less than the value of the time constant k_{ST} for S – T transitions in the EHP (Fig. 1.12). Therefore, for large values of E, triplet EHPs dissociate earlier than the spin conversion occurs and the influence of an external magnetic field on the photocurrent will manifest.

In accordance with the hyperfine interaction mechanism, the negative effect δ_- in PEPC films with CICT3 is caused by the fact that at distances between the charges in the EHP close to r_C (but not smaller) the EHPs are mainly singlet. An external magnetic field at $r \geq r_C$ makes it impossible to establish an equilibrium distribution of the concentration of EHP over spin states and shifts the distribution of EHP towards an increase in the concentration of singlet EHP. This

leads to a decrease in the concentration of triplet EHPs dissociating in an external electric field, and to the negative effect δ_- (Fig. 1.23). The manifestation of both positive δ_+ and negative δ_- effects depending on the value of E in PEPC films with CICT2 (Fig. 1.22) can be interpreted by using assumptions in explanation the effects of δ_+ in PEPC films with CICT1 and δ_- in PEPC films with CICT3. Consequently [181,184–186], in the PEPC films with SVPZ2, at distances between the charges in the EHP close to r_C (but not smaller), concentrations of both triplet and singlet EHP are present simultaneously. Only a positive effect is observed in PEPC films with CICT1 where r_0 has the highest value of 12.4 Å and close to r_C = 15 Å. Only a negative effect is observed in PEPC films with CICT3 where r_0 has the smallest value of 8.3 Å.

One can make an assumption regarding the multiplicity of the generated EHPs and the evolution of the multiplet state in the process of increasing the distance from the charges from r_0 to r_C. This assumption consists in the fact that, as a result of the thermalization of the charge carrier, triplet EHPs are formed from the excited CICT molecule with distances between the charges $r = r_0$. With an increase in the distance between the charges in the EHP to $r = r_C$, there is a probability of a change in the multiplicity of the EHP as a result of the hyperfine interaction mechanism and at distances between the charges $r < r_C$ [167–169]. This probability is the greater, the longer the movement of charges from r_0 to r_C and the greater the difference $r_C - r_0$.

The greatest probability of changing the multiplicity is in EHP in PEPC films with CICT3. Under these assumptions regarding the peculiarities of the manifestation of the positive and negative effects of the magnetic field on the photogeneration efficiency, differences in the frequency factors of hole tunneling between carbazole fragments and the donor parts of the CICT molecules can be explained. For recombination of charges in an EHP with $r = r_0$, it is necessary to change the multiplicity of the EHP from triplet to singlet. The probability of this process at $r = r_0$ depends on the value of the energy of the exchange interaction of spin charges in the EHP, and the larger it is, the larger r_0 is. In expression (1.16) for the charge recombination time constant τ_a this probability is taken into account in ν_1 and determines its value. Consequently, the value ν_1 will be the

largest for PEPC films with CICT1, smaller for PEPC films with CICT2, and the smallest for films with CICT3 which is confirmed experimentally. To test the validity of this assumption regarding the possible mechanism of the influence of H on the efficiency of photogeneration of charge carriers, we calculated the dependency of δ_+ and δ_- on E as a result of solving the system of continuity equations [181, 184–186].

$$\partial n_3/\partial t = G(1-f) - n_3(1/\tau_\eta + 1/3\tau_{ST}) + n_1/\tau_{ST}, \quad (1.17)$$

$$\partial n_1/\partial t = Gf - n_1(1/\tau_\eta + 1/\tau_a + 1/\tau_{ST}) + n_3/3\tau_{ST}, \quad (1.18)$$

where G is the photogeneration efficiency of triplet EHPs; f is the probability of a change in the multiplicity of triplet EHPs with increasing distance between charges in an EHP from r_0 to r_C; n_3 and n_1 are, respectively, the concentrations of triplet and singlet EHPs with distances between the charges $r \geq r_C$. For the stationary case $\partial n_3/\partial t = \partial n_1/\partial t$, $j_{PH} \sim (n_1 + n_3)/\tau_\eta$ and the conditions τ_{ST}, τ_a, $\tau_\eta \ll \tau_{ST}(H)$ ($\tau_{ST}(H)$ is the time constant of singlet-triplet transitions in an external magnetic field H), the relative change in δj_{PH} can be represented as:

$$\delta j_{PH} = \{3f\tau_\eta^{-1} - (1-f)(\tau_\eta^{-1} + \tau_a^{-1})\tau_a^{-1}\}/\{f(\tau_\eta^{-1} + 4\tau_{ST}^{-1}) + (1-f)(\tau_\eta^{-1}+\tau_a^{-1}+4\tau_{ST}^{-1}\}\cdot\tau_{ST}^{-1}/\{(\tau_\eta^{-1}+\tau_a^{-1})\tau_\eta^{-1}+(\tau_a^{-1}+4\tau_\eta^{-1})\tau_{ST}^{-1}\}. \quad (1.19)$$

When calculating the dependency of δj_{PH} on E, the value τ_{ST} was determined [113] from the following expression

$$\tau_{ST} = \hbar/(g_s\mu_B H_A). \quad (1.20)$$

The value of H_A corresponds [168] to the value of the external magnetic field strength when the δj_{PH} value in the dependency δj_{PH} on H is half of the saturation value of this dependency. For such an approximation, $\tau_{ST} = 2 \cdot 10^{-9}$ s. The value of $\tau_{ST}(H)$ was considered close to $(T_1^{-1} + T_2^{-1})^{-1}$, where T_1 and T_2 are the spin-lattice and spin-spin relaxation times, respectively, calculated using following expressions [188]:

$$T_1 = 1.97 \cdot 10^{-7}\Delta H_{pp}/g_s H_1^2, \quad (1.21)$$

$$T_2 = 1.3131 \cdot 10^{-7}/g_s\Delta H_{pp}. \quad (1.22)$$

Here, ΔH_{pp} is the width of the EPR signal between the points of its maximum slope, H_1 is the amplitude value of the magnetic field of the microwave pumping corresponding to the maximum amplitude

value of the EPR signal [168,188]. From measurements of the EPR signal (insert in Fig. 1.20), the values of T_1 and T_2 are $4 \cdot 10^{-5}$ s and $8 \cdot 10^{-8}$ s, respectively. The results of numerical simulation [181, 184–186] of the dependencies $\delta j_{PH}(E)$ are presented in Fig. 1.21–Fig. 1.23 by curves *4*. The value of f was changed from 0 to 1 and was a simulation parameter. Experimentally obtained and calculated according to (1.19) dependencies $\delta j_{PH}(E)$ for PEPC films with CICT1 and f = 0.25 (Fig. 1.21), PEPC with CICT2 and f = 0.8 (Fig. 1.22), PEPC with CICT3 and f = 0.95 (Fig. 1.23) correlate. The qualitative correspondence of the results of experimental investigations and numerical calculations using a simplified model indicates the admissibility of assumptions about the initial spin state of an EHP and its changes in the process of dissociation of EHP into current carriers.

The initial triplet state of an EHP is not a prerogative of the FPC with a CICT but is of a more fundamental nature caused by the peculiarities of the intramolecular conversion of photogeneration centers. This is confirmed, in particular, by the results of studies [189] of the photoconductive properties of heterostructures from PEPC and [2-methoxy-5-(2′-ethylhexyloxy)-1,4-phenylene-vinylene] films (MEH-PPV) doped with 2,3,9,10,16,17,23,24-octabutylphthalocyanine zinc (PcBuZn) in the absorption range of the metal complex.

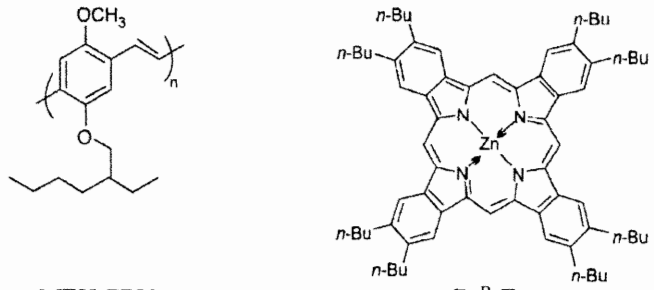

MEH-PPV $Pc^{Bu}Zn$

Fig. 1.25. shows the results of measurements of the dependency of j_{PH} on E. In double logarithmic coordinates, the graphs of this dependency can be approximated by straight lines making it possible to describe it with the analytical expression $j_{PH} \sim E^m$

The value of the exponent m > 2 and it does not depend on the polarity of U. But the value of j_{PH} increases at the transition from

samples ITO – MEH-PPV + 3 wt.% $Pc^{Bu}Zn$ – Ag to samples ITO – MEH-PPV + 3 wt.% $Pc^{Bu}Zn$/PEPC – Ag, ITO – PEPC/MEH-PPV + 3 wt.% $Pc^{Bu}Zn$ – Ag, and in the latter two cases it significantly depends on the polarity of U. This means that the photoconductive properties of the investigated heterostructures, in contrast to samples with MEH-PPV + 3 wt.% $Pc^{Bu}Zn$, are sensitive to the polarity of the applied electrical voltage.

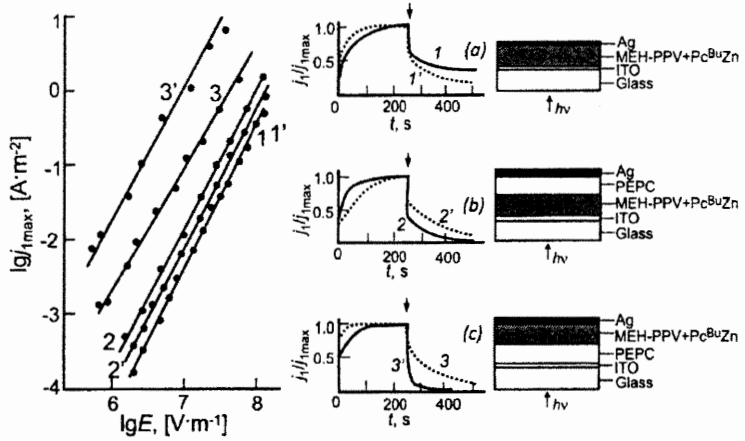

Fig. 1.25. Dependencies of lgj$_{PH}$ on lgE in samples with ITO – MEH-PPV + 3 wt. % $Pc^{Bu}Zn$ – Ag (*1*, *1'*), ITO – MEH-PPV + 3 wt.% $Pc^{Bu}Zn$ /PEPC – Ag (*2*, *2'*), ITO – PEPC/MEH-PPV + 3 wt.% $Pc^{Bu}Zn$ – Ag (*3*, *3'*) with a positive (*1 – 3*) and negative (*1' – 3'*) polarity U on the ITO electrode, as well as a cross-section image of the investigated samples. Light intensity 20 W/m^2

To establish the reason for the increase in j_{PH} at the transition from samples with ITO – MEH-PPV + 3 wt.% $Pc^{Bu}Zn$ – Ag to samples with ITO – PEPC / MEH-PPV + 3 wt.% $Pc^{Bu}Zn$-Ag were investigated [189] the features of the photogeneration of an electron-hole pair and the transport of non-equilibrium current carriers. Fig. 1.26 shows the graphs of the dependency δj_{PH} (H). The rapid increase in j_{PH} after switching on the magnetic field and a small change in δj_{PH} for H > 1 kOe indicates that triplet EHPs are mainly formed at the first stage of photogeneration. In this case, switching on and off of H does not affect the current of electrical conductivity.

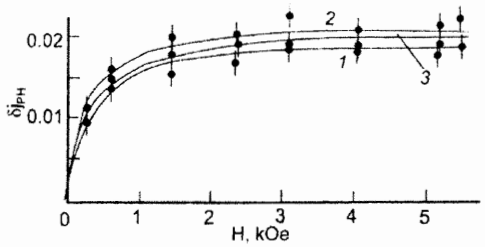

Fig. 1.26. Dependencies $\delta j_{PH}(H)$ in samples with ITO – MEH-PPV + 3 wt.% $Pc^{Bu}Zn$ – Ag (*1*), ITO – MEH-PPV + 3 wt.% $Pc^{Bu}Zn$ / PEPC – Ag (*2*), ITO – PEPC / MEH-PPV + 3 wt.% $Pc^{Bu}Zn$ – Ag (*3*)

Usually, EHPs are formed in FPC from singlet excited states of dye molecules or related compounds. However, the presence of metal ions, other high-spin particles, or halogens [190–194] may contribute to spin conversion. Since the graphs of $\delta j_{PH}(H)$ dependencies differ little for the studied FPC, the conclusion [189] was made that the presence of a heterojunction in FPC has little effect on the spin state of EHP. After the formation of mobile charge carriers as a result of the dissociation of long-lived EHPs, they (charge carriers) can get into energy traps near the photogeneration centers i.e. near $Pc^{Bu}Zn$ molecules. Thus, $Pc^{Bu}Zn$ molecules can simultaneously be considered [189] both as photogeneration centers and as catalysts for spin conversion of EHPs. In this connection, the question of the possibility of separating spin-dependent processes at the stages of the formation and dissociation of EHP becomes interesting.

1.5. Spin conversion in electron-hole pairs

As can be seen from the above, the mechanism of photogeneration of charge carriers in an FPC consists of 2 stages [95, 101]. At the first stage of photogeneration, an EHP forms after absorption of a light quantum in the photogeneration center. On the second stage after the formation of an EHP, charge carriers that are part of an EHP can either